**Democratic and Popular Republic of Algeria**
**Ministry of Higher Education and Scientific Research**
**Chadli Bendjedid University – El Tarf**
**Faculty of Sciences and Technology**
**Process Engineering Department**

## Professional Master's Thesis

**Field:** Sciences and Technology

**Major:** Process Engineering

**Specialty:** Water Treatment and Desalination

**Theme:**

# Synthesis and Application of Bio-nanomaterials for Water Treatment

**Presented by:**

**BARKAT Lobna**

**Defended on: 17/06/2026 before the Jury:**

| | | | |
|---|---|---|---|
| **Dr. OUCHEN Abdelali** | **President** | **MCB** | **Univ. El-Tarf** |
| **Dr. BELAIDI Ouafa** | **Supervisor** | **MCB** | **Univ. El-Tarf** |
| **Dr. Bekakria. Hamida** | **Co-Supervisor** | **MCB** | **Univ. El-Tarf** |
| **Dr. AITBARA Adel** | **Examiner** | **MCA** | **Univ. El-Tarf** |

**Academic Year: 2025/2026**

# Dedication

I dedicate this modest work to:

My beloved parents, who have given me everything and have always ensured that I never lacked anything. For their sacrifices, unwavering support, encouragement, and unconditional love.

I hope that one day I will be able to repay even a small part of all that they have done for me.

May God bless them with happiness, good health, and a long life. I also dedicate this work to my dear brother, Adam, and my dear sister, Hiba, for their affection, presence, and constant support.

To my dear friends, Aya and Khawla, for their encouragement, valuable assistance, and for all the memorable moments we shared throughout this journey.

To my entire family, for their love and continuous encouragement.

Finally, I dedicate this work to all the teachers and professors who contributed to my education and guided me throughout my academic journey.

I would also like to extend my sincere appreciation to all my classmates, with whom I shared years of learning, hard work, and perseverance.

To everyone who contributed, directly or indirectly, to the completion of this work, I express my heartfelt gratitude.

*Lobna*

# Acknowledgment

This work was carried out partly at the Mexa water treatment plant, as well as in several university laboratories that contributed to the completion of the necessary analyses.

First, I would like to express my sincere thanks to **Dr. BELAIDI Ouafa**, as supervisor, for accepting to supervise this work.

I would also like to thank Mrs. **BEKAKRIA Hamida**, co-supervisor, for her guidance and support throughout this work.

I would also like to express my deep gratitude to **YOUBI Asma**, for her welcome at the Mexa water treatment plant, her field guidance, her constant availability, her valuable support, and her help throughout all the practical stages of this work. Her involvement was essential to the completion of this thesis.

My sincere thanks go to the members of the examination committee, **namely Dr. AITBARA Adel** and **Dr. OUCHEN Abdelali**, for agreeing to evaluate this work.

I would also like to thank Mrs Derradji and Tigrine for their valuable help and collaboration during the practical part of this work.

Finally, I would like to express my gratitude to all those who, directly or indirectly, contributed to this work.

# Table of Contents

## List of Figures

## List of Tables

# List of Abbreviations

AOPs Advanced Oxidation Processes

AC Activated Carbon

$BOD_5$ Biochemical Oxygen Demand

COD Chemical Oxygen Demand

CM Cistus monspeliensis

CMLE Cistus monspeliensis Leaf Extract

EC Electrical Conductivity

EDL Electrical Double Layer

Fe Iron

FeNPs Iron Nanoparticles

$Fe_3O_4$ Magnetite

$FeCl_3$ Ferric Chloride

$FeSO_4$ Ferrous Sulfate

LiOH Lithium Hydroxide

NaOH Sodium Hydroxide

$NP_{Fe}$ Iron Nanoparticles used as Bio-coagulant

NPs Nanoparticles

NTU Nephelometric Turbidity Unit

PAC Poly Aluminum Chloride

pH Potential of Hydrogen

ROS Reactive Oxygen Species

SS Suspended Solids

STEP Station de Traitement des Eaux Usées

TAC / TA Total Alkalinity

TDS Total Dissolved Solids

UV Ultraviolet

XRD X-Ray Diffraction

DRX Diffraction des Rayons X

ZnO Zinc Oxide

$TiO_2$ Titanium Dioxide

CdS Cadmium Sulfide

MRI Magnetic Resonance Imaging

E. coli Escherichia coli

$NO_2^-$ Nitrite

$NO_3^-$ Nitrate

$PO_4^{3-}$ Phosphate

$OH^-$ Hydroxide Ion

$HCO_3^-$ Bicarbonate Ion

$CO_3^{2-}$ Carbonate Ion

$O_2$ Oxygen

$CO_2$ Carbon Dioxide

$H_2O$ Water

# Introduction

surface waters and wastewater are currently among the most environmentally vulnerable compartments, increasingly exposed to growing levels of pollution primarily driven by industrial, agricultural, and domestic discharges. This progressive contamination leads to a significant deterioration in water quality, directly impacting aquatic ecosystems and human health, particularly due to the presence of persistent organic compounds, heavy metals, and emerging micropollutants [1].

Despite the existence of conventional treatment processes such as coagulation–flocculation, sedimentation, and biological treatments, their efficiency is sometimes limited when facing the complexity and diversity of modern pollutants. Indeed, certain contaminants are resistant to classical treatment methods or require strict operational conditions, thereby reducing the overall performance of wastewater treatment plants [2].

In response to these limitations, scientific research has increasingly turned toward more advanced technologies, particularly advanced oxidation processes and heterogeneous photocatalysis. These techniques rely on the generation of highly reactive species capable of effectively degrading recalcitrant organic pollutants, offering a promising alternative for improving water quality [3].

Moreover, the integration of nanomaterials into water treatment has opened new perspectives. Owing to their high specific surface area and unique physicochemical properties, nanoparticles (such as metal oxides) significantly enhance adsorption, catalytic reactions, and pollutant degradation processes [4]. In this context, the combination of photocatalysis and nanotechnology represents an innovative, sustainable, and highly efficient approach to addressing current challenges in water treatment [5].

Therefore, the development of advanced photocatalytic materials based on nanostructured systems constitutes a promising solution to overcome the limitations of conventional methods and to enhance the overall efficiency of water purification systems [6].

# Chapter I

# Bibliographic Research

## I.1. water pollution

Water pollution is defined as any undesirable modification of the natural properties of water resulting from the introduction of contaminants that alter its physical, chemical, or biological characteristics, leading to a deterioration in its quality and ecological status. It adversely affects aquatic environments, disrupts ecosystem balance, and reduces the suitability of water resources for various uses.[7]

**Figure I- 1 Water pollution resulting from wastewater discharge.[8]**

## I.2. Classification of Pollutants

Water pollutants can be categorized into different groups based on their origin, composition, and environmental effects. The main classifications are presented in Table I-1.

**Table I- 1. Classification of Major Water Pollutants**

| TYPE OF POLLUTANT | DESCRIPTION | EXAMPLES |
|---|---|---|
| **CHEMICAL** | Presence of undesirable or hazardous dissolved substances in excess or outside their normal environment | Dissolved chemical compounds [9] |
| **RADIOACTIVE** | Pollution caused by the release of radioactive elements from nuclear, medical, and industrial activities | Nuclear explosions, atomic wastes, radioisotopes [9] |
| **BIOLOGICAL** | Presence of free-living or pathogenic organisms in water. | Plankton, macro-invertebrates, microorganisms,protozoa, bacteria, viruses [9] |
| **PHYSICAL** | Solid elements transported by water, classified according to their nature and size. | Twigs, leaves, sands, suspended solids [9] |

To evaluate the extent of water contamination, water quality is assessed through a set of physical, chemical, and microbiological parameters. These indicators provide quantitative and qualitative information about the state of water and are widely used to determine its suitability for different uses and to monitor treatment efficiency

## I.3. Physicochemical characteristics:

### I.3.1. Temperature

Water temperature depends on daily or seasonal variations in ambient temperature, as well as on anthropogenic discharges (e.g., water used for cooling). This parameter plays an important role in the functioning of aquatic ecosystems through its influence on the solubility of oxygen as well as other elements.[10]

### I.3.2. pH

pH is the negative logarithm of hydrogen ion concentration and indicates the acidity or alkalinity of a water sample. It is a key parameter in water quality assessment and is closely

related to corrosivity and electrical conductivity. Variations in pH are mainly controlled by physicochemical conditions and may result from anthropogenic inputs such as industrial discharges, acid rain, and organic matter decomposition.[11]

### I.3.3. Turbidity

Turbidity is the cloudiness of water caused by suspended and colloidal particles such as clay and organic matter. These particles can transport microorganisms and adsorb pollutants including heavy metals and organic compounds. High turbidity may increase water temperature and reduce dissolved oxygen levels. It is measured in NTU using a nephelometric turbidimeter, where high values indicate poor water quality.[12]

### I.3.4. Suspended solids (SS)

Suspended solids include all mineral or organic matter that does not dissolve in water. They include clays, sands, silts, small-particle organic and mineral matter, plankton, and other aquatic microorganisms. The number of suspended solids varies significantly depending on the season and the water flow regime. These materials affect water clarity and reduce light penetration, thereby hindering photosynthesis. They can also interfere with fish respiration. Furthermore, suspended matter can accumulate high levels of toxic substances (metals, pesticides, mineral oils, polycyclic aromatic hydrocarbons, etc.) [13]

### I.3.5. Salinity and Electrical Conductivity

Salinity refers to the concentration of dissolved salts in water, while electrical conductivity (EC) reflects its overall ionic content. Salts dissociate in water into charged ions that determine its conductivity.

Salinity is classified into primary, originating from natural processes such as rock weathering and long-term salt deposition, and secondary, mainly resulting from human activities like land clearing and improper land use, which lead to salt accumulation and disruption of natural water systems.

Electrical conductivity is influenced by dissolved ions (e.g., $Ca^{2+}$, $Na^{+}$, $Cl^{-}$, $SO_4^{2-}$, $NO_3^{-}$), organic compounds, and physico-chemical parameters such as pH, total hardness, total solids, TDS, and COD. Temperature also affects EC by increasing ion mobility and dissociation while reducing water viscosity.[14]

### I.3.6. Alkalinity

Alkalinity is the capacity of water to neutralize hydrogen ions ($H^+$) and resist changes in PH. It is mainly attributed to the presence of bicarbonate ($HCO_3^-$), carbonate ($CO_3^{2-}$), and hydroxide ($OH^-$) ions.[15]

### I.3.7. Biochemical Oxygen Demand (BOD)

Biochemical oxygen demand is, by definition, the amount of oxygen required by living microorganisms present in the environment to ensure the oxidation and stabilization of organic matter in water. By convention, BOD is the value obtained after five days of incubation, BOD5 [16]

### I.3.8. Chemical Oxygen Demand (COD)

This is the amount of oxygen required for the chemical breakdown of oxidizable organic matter in water. Certain organic substances are difficult for microorganisms to biodegrade, and a strong chemical oxidizing agent is required to oxidize them; the chemical oxygen demand determines the total amount of oxygen needed to break down the pollution. COD is also expressed in mg O2/L. [17]

## I.4. Microbiological parameters:

### I.4.1. Total bacteria

These bacteria grow under aerobic conditions. Their presence indicates bacterial contamination. Counting them provides information on the hygienic quality of water intended for human consumption [18] Thus, they provide information on the degree of protection of groundwater aquifers [19].

### I.4.2. Coliforms

Coliforms belong to the Enterobacteriaceae family; these coliform bacteria are rod-shaped, non-spore-forming, Gram-negative, oxidase-negative, facultative aerobes and anaerobes, capable of fermenting lactose to produce acid and gas within 48 hours at temperatures of 35 and 37°C. Coliforms include the genus: Escherichia coli.[20]

### I.4.3. Fecal coliforms or thermotolerant coliforms

Fecal coliforms are coliforms that exhibit the same properties (characteristic of coliforms) after incubation at a temperature of 44°C. [21]

### I.4.4. Fecal streptococci

Fecal streptococci are generally considered to be indicators of fecal contamination. They are Gram-positive, chain-forming, facultative anaerobes, and non-motile).[18]

## I.5. Undesirable or Toxic Parameters

### I.5.1. Ammonium

Ammonium mainly originates from the decomposition of nitrogen-rich organic matter as well as industrial activities such as fertilizers and textiles. It plays an important role in the nitrogen cycle and can exist in water either in molecular form (ammonia) or as the ionized form depending on pH conditions.[22]

### I.5.2. Iron

Iron is naturally present in groundwater due to its abundance in the Earth's crust. Its concentration in water is influenced by geological conditions, soil leaching, industrial discharges, and corrosion of distribution pipes.[18]

### I.5.3. Aluminum

Aluminum is also widely distributed in the environment. In acidic conditions, it exists in dissolved ionic form ($Al^{3+}$). Although generally not harmful at low concentrations, its presence in water is considered undesirable when elevated.[23]

### I.5.4. Nitrites

Nitrites are intermediate compounds in the nitrogen cycle, formed either by incomplete oxidation of ammonia or by reduction of nitrates under anaerobic conditions. Their occurrence in water is usually limited and associated with specific pollution processes.[24]

### I.5.5. Nitrates:

Nitrates represent the final product of nitrogen oxidation. They are highly soluble and commonly found in water due to agricultural activities, organic waste, and wastewater discharges.[25]

### I.5.6. Phosphates

Phosphates in water often indicate contamination from agricultural runoff or surface infiltration. In natural, unpolluted waters such as springs and deep groundwater, their presence is typically very low.[26]

## I.6. Water Treatment Methods

Water treatment technologies can be classified into different categories based on the type of process applied, such as physical, chemical, and biological treatments. The main methods are listed in the table below

**Table I- 2 Comparison Water Treatment Methods**

| | |
|---|---|
| **Physical treatment** | **Screening, sedimentation, filtration, flotation, membrane separation, granular media, flow equalization [27]** |
| **Chemical treatment** | Coagulation, chemical precipitation, ion exchange, adsorption, neutralization, solvent extraction, chlorination, other chemical applications [28] |
| **Biological treatment** | Aerobic digestion, anaerobic digestion, activated sludge process, bacterial filters, rotating biological contactors, pond stabilization, biological nutrient removal.[28] |

### I.6.1. Coagulation–Flocculation

The turbidity of surface water is caused by the presence of very small particles known as colloids. Their removal cannot rely on simple settling, as their sedimentation rate is extremely low. The time required for a particle to fall freely over a distance of one meter can reach several years. Coagulation–flocculation is a physicochemical process aimed at destabilizing colloidal particles present in water, followed by the formation of flocs through adsorption and aggregation. The flocs formed are subsequently removed by sedimentation and filtration [29]

#### I.6.1.1. Coagulation

Coagulation is the first stage of the coagulation–flocculation process. It involves the destabilization of suspended colloidal particles through the neutralization of their electrical charges by the addition of chemical substances known as coagulants. These colloidal particles generally carry a negative electrical charge, which generates repulsive forces that prevent their approach and aggregation.

According to the electrical double layer theory, an ionic environment forms around colloidal particles. Positively charged ions in water accumulate at the colloid surface, forming the Stern layer. Beyond this layer lies the diffuse layer (Gouy layer), which consists of more randomly distributed ions.

The boundary between these two layers is called the shear plane. The electrical potential measured at this level is known as the zeta potential, which serves as an indicator of colloidal stability. The ionic strength of the medium also influences the electrostatic behavior of the particles. The addition of a coagulant increases the ionic concentration, leading to compression of the electrical double layer and a reduction in repulsive forces. Consequently, van der Waals forces become dominant, promoting particle aggregation. [30]

Colloidal destabilization can occur through four main mechanisms:

- Double layer compression
- Adsorption and charge neutralization
- Enmeshment in a precipitate
- Adsorption and bridging between particles. [31]

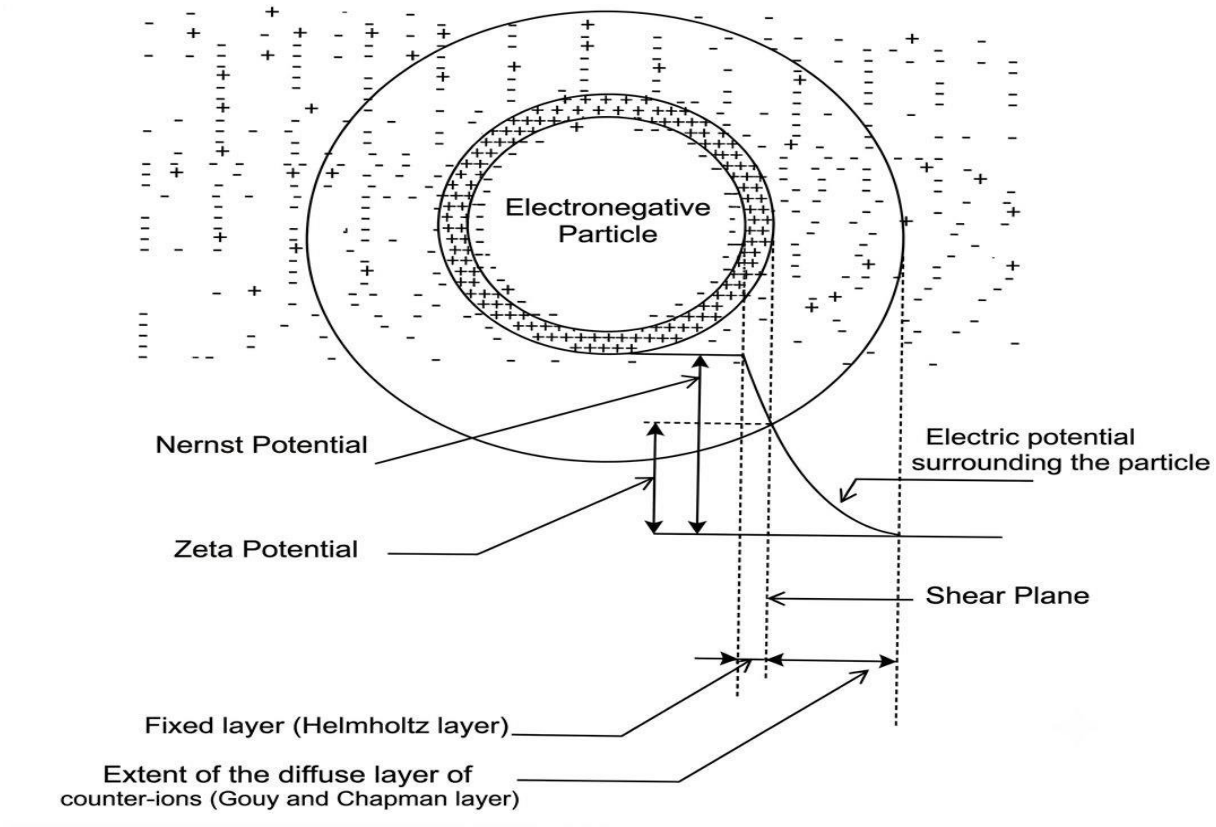


**Figure I- 2 Structure of the electrical double layer (EDL) showing the Stern layer, diffuse layer, and zeta potential around a negatively charged particle.[32]**

### I.6.1.2. Types of Coagulants Commonly Applied in Water Treatment

**Table I- 3Types of Coagulants Used in Water Treatment [31]**

| Coagulant type | Examples |
|---|---|
| **Inorganic coagulants** | Aluminum sulfate ($Al_2(SO_4)_3$), Ferric chloride ($FeCl_3$), Ferric sulfate ($Fe_2(SO_4)_3$), Poly aluminum chloride (PAC) |
| **Organic coagulant** | Polyamines, PolyDADMAC |
| **Bio-coagulants** | Chitosan, starch, tannins, plant extracts |

### I.6.2. Flocculation

Flocculation involves the addition of high-molecular-weight polymers to promote the aggregation of colloidal particles. This process is mainly based on two mechanisms: interparticle bridging, in which polymer chains connect several particles together, and charge

neutralization, which reduces electrostatic repulsion and enhances the formation of larger flocs.**[33]**

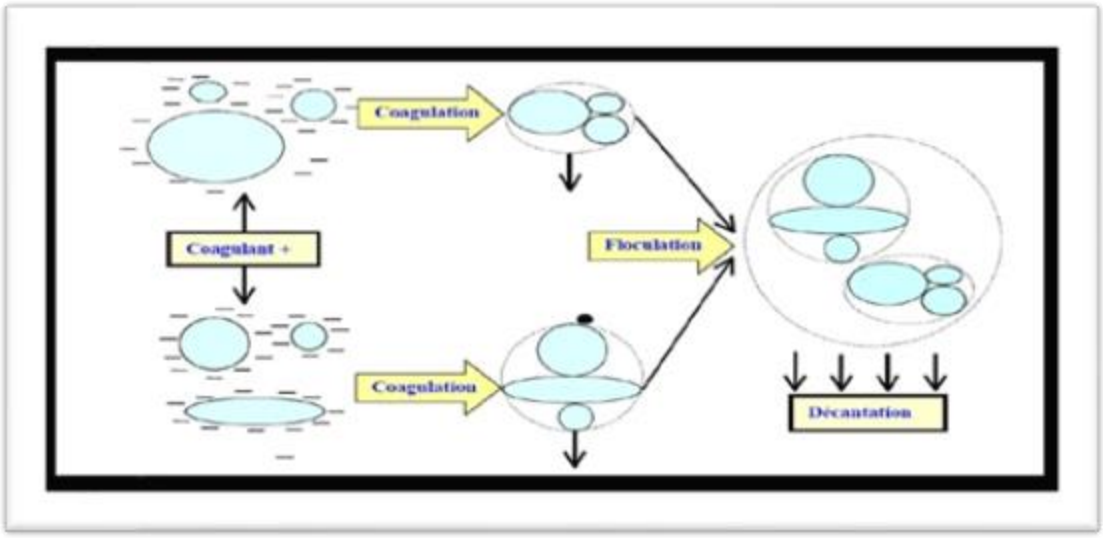


**Figure I-3. Schematic illustration of the coagulation–flocculation and sedimentation processes in water treatment.[34]**

### I.6.2.1. Types of flocculants Used in Water Treatment

**Table I- 4. Types of Flocculants Used in Water Treatment [33]**

| Type | Examples |
|---|---|
| **Organic flocculants** | Starch, alginates, polysaccharides |
| **Mineral flocculants** | Activated silica, bentonite, alumina, ferric hydroxide, fine sand |
| **Synthetic flocculants** | Polyacrylamide, acrylamide + acrylic acid, acrylamide + methacrylate |

Conventional water treatment methods are effective for the removal of particulate matter and macroscopic parameters; however, they present significant limitations in the removal of micropollutants and dissolved organic matter. They may also lead to the formation of disinfection by-products and often require additional treatment steps to ensure water safety.[35]

### I.6.3. Advanced oxidation processes (AOPs):

Currently, advanced oxidation processes (AOPs) are widely used for the treatment of contaminated water. They rely on the generation of hydroxyl radicals (•OH), highly reactive species capable of effectively degrading a wide variety of organic pollutants.

The primary objective of these processes is to transform pollutants into simpler compounds, and ideally to mineralize them into carbon dioxide ($CO_2$) and water ($H_2O$).

AOPs encompass several techniques based on different oxidation sources and activation modes, which give them a wide range of applications in water treatment.

These processes are notably used to reduce pollutant load and toxicity and to improve the overall quality of effluents by promoting the degradation of organic compounds.[36] [37]

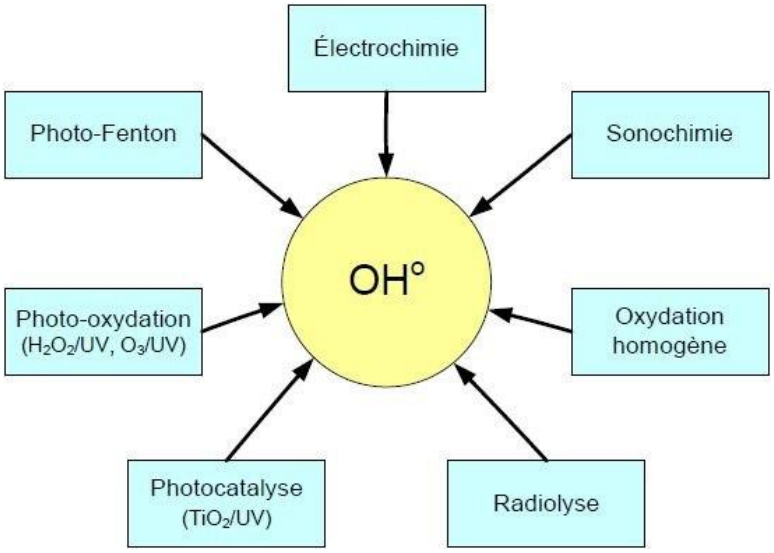


**Figure I- 3. Methods of hydroxyl radical (OH) formation. [38]**

Among the different advanced oxidation processes, photocatalysis is commonly regarded as one of the main oxidation techniques used in water treatment. Photocatalysis

### I.6.4. Photocatalysis

is a light-driven catalytic process in which a photoactive material absorbs photons and promotes chemical transformations without being consumed during the reaction. It can be classified into homogeneous and heterogeneous photocatalysis. In homogeneous systems, the catalyst and reactants are present in the same phase, whereas in heterogeneous systems they

exist in different phases. Due to its simplicity, stability, and ease of catalyst recovery, heterogeneous photocatalysis is the most widely applied approach in water treatment. **[39][40]**

### I.6.4.1. Heterogeneous photocatalysis

Heterogeneous photocatalysis involves a solid semiconductor catalyst interacting with pollutants present in the aqueous phase. Upon illumination with light of sufficient energy, a series of oxidation–reduction reactions take place at the catalyst surface, resulting in the degradation and transformation of contaminants.**[41]**

### I.6.4.2. Reaction mechanism

The photocatalytic process includes several successive steps: transfer of reactants toward the catalyst surface, adsorption of pollutants, surface reactions, desorption of products, and their diffusion back into the solution. When the semiconductor absorbs photons with energy equal to or greater than its band-gap energy, electrons are promoted from the valence band to the conduction band, generating electron–hole pairs ($e^-/h^+$). These charge carriers subsequently react with water, hydroxide ions, and dissolved oxygen to produce reactive oxygen species (ROS), mainly hydroxyl radicals (•OH) and superoxide radicals ($O_2•^-$), which are responsible for the degradation of organic pollutants**.[42]**

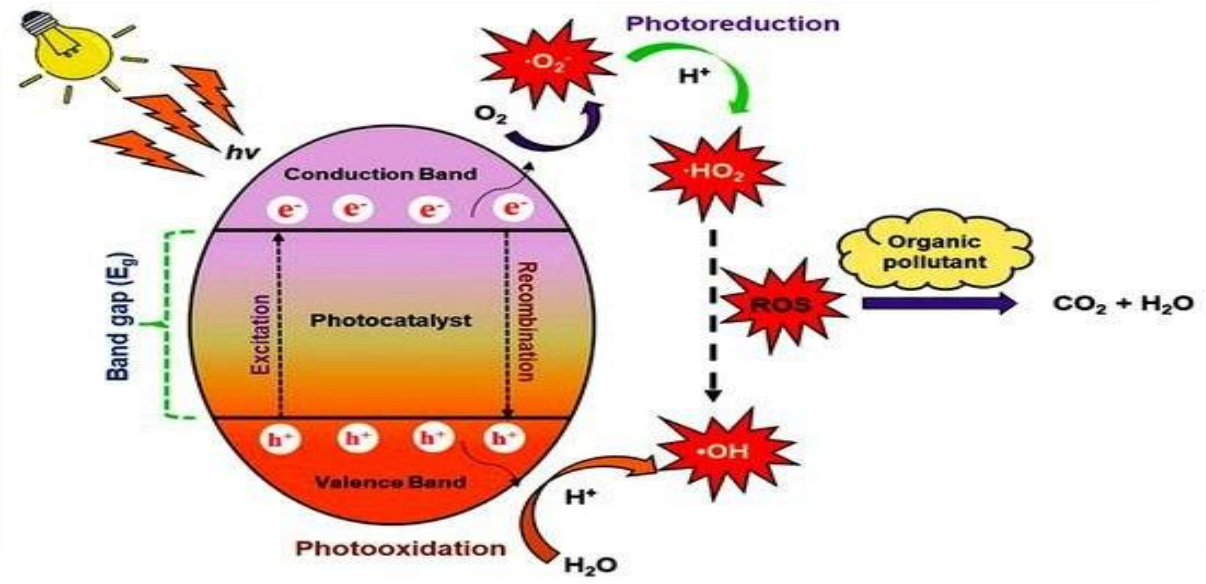


**Figure I- 4. Schematic mechanism of heterogeneous photocatalysis for organic pollutant degradation [43]**

### I.6.4.3. Photocatalysts

Photocatalysts are photoactive semiconductor materials capable of converting light energy into chemical energy. Their efficiency depends on several factors, including light absorption capacity, charge separation efficiency, and resistance to electron–hole recombination. Among the most commonly used photocatalysts are $TiO_2$, ZnO, and CdS, owing to their favorable electronic properties, chemical stability, and high photocatalytic activity. **[44]**

### I.6.4.4. Factors influencing photocatalysis

The efficiency of heterogeneous photocatalysis is influenced by several operational parameters:

- **Initial pollutant concentration:** An increase in the initial concentration of the pollutant generally leads to a decrease in photocatalytic efficiency, as higher pollutant levels hinder light penetration to the catalyst surface and consequently reduce the degradation of contaminants.[45]

- **Catalyst concentration:** the reaction rate increases with catalyst loading up to an optimum value, beyond which light scattering and shielding effects may reduce efficiency.[46]
- **pH of the medium**: affects both the surface charge of the catalyst and the adsorption behavior of pollutants.**[47]**.
- **Light intensity**: controls the generation rate of charge carriers and consequently the photocatalytic activity.
- **Irradiation wavelength**: must match the absorption characteristics of the semiconductor.
- **Electron acceptors**: species such as oxygen or hydrogen peroxide improve charge separation and limit electron–hole recombination.[48]

### I.6.4.5. Applications of photocatalysis in water treatment

- **Degradation of organic pollutants (including dyes and industrial chemicals)**

Photocatalysis is widely used for the degradation of organic pollutants in water such as industrial chemicals, pesticides, and synthetic dyes. Under light irradiation, reactive oxygen species (ROS) are generated on the photocatalyst surface, which oxidize and break down complex organic molecules into simpler and less toxic compounds. In the case of textile dyes, the process leads to destruction of chromophoric structures responsible for color, resulting in decolorization and degradation.[49]

- **Treatment of toxic and recalcitrant organic compounds (hydrocarbons and phenolic compounds)**

Photocatalysis is effective in the treatment of petroleum hydrocarbons and phenolic compounds in contaminated water. These pollutants are resistant to conventional treatment methods; however, photocatalytic oxidation promotes the cleavage of carbon chains and aromatic rings, significantly reducing toxicity and environmental impact.[50]

- **Complete mineralization and water purification**

One of the main advantages of photocatalysis is the complete mineralization of organic pollutants into carbon dioxide and water without producing harmful intermediates. It is also used for the purification of surface water and groundwater by removing persistent and non-biodegradable contaminants.[51]

Recently, nanomaterials have attracted considerable attention in water treatment owing to their large specific surface area, enhanced reactivity, and improved photocatalytic performance, making them promising candidates for advanced environmental remediation applications.

## I.7. General information on nanomaterials

Nanotechnology and nanoscience study the properties of systems with dimensions ranging from a few angstroms to a hundred nanometers. Nanomaterials establish a space for research and development involving the use of processes that allow the organization of matter at the molecular or atomic level at characteristic scales from 1 to 100 nanometers (nm).

Materials are produced from the destruction of a macroscopic material, or by the arrangement of a group of atoms or molecules. These nanoparticles can have different forms (nano-spheres, nanotubes, nano-wires, cells, single crystals...). Nanomaterials have different characteristics from the macroscopic scale, thanks to their size. Certainly, as the size of a particle decreases, the number of particles per unit mass increases. Nanoparticles have properties that depend on their sizes due to the large proportion of existing atoms on their surfaces relative to their volumes, which results in a high specific surface area. [52].

Nanoscale structures then make it possible to obtain new materials with particular mechanical, electrical, magnetic, optical and catalytic properties that sometimes differ from the properties of the same material on a different scale. [53].

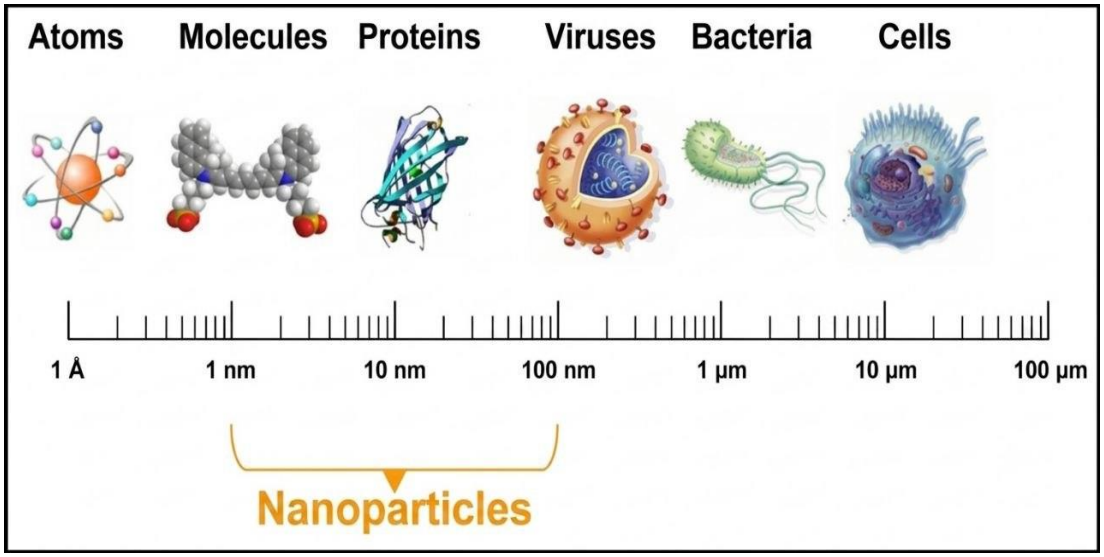


**Figure I- 5. Comparison of the size of nanoparticles with biological and chemical entities on the nanometer scale (Created using Bio Render).[54]**

### I.7.1. Definition of a nanoparticle

A nanoparticle is an ultrafine particle composed of atoms or molecules with dimensions generally ranging from 1 to 100 nm. Due to their nanoscale dimensions, nanoparticles exhibit unique physicochemical properties that distinguish them from their bulk counterparts. Their size is comparable to that of biological entities such as proteins and viruses [55].

## I.8. Methods of nanoparticles synthesis:

### I.8.1. The top-bottom/mechanical production method

The top-down (mechanical) production method is based on the reduction of bulk materials into nanoparticles through mechanical processes such as milling and crushing. It commonly involves high-energy ball milling of metallic oxides as starting materials [56–57]. The process is performed using high-hardness steel equipment to achieve efficient grinding and particle size reduction [58].

### I.8.2. The bottom-up/chemical production method

The bottom-up method is based on the synthesis of nanoparticles from atoms or molecules through chemical reactions such as co-precipitation, condensation, and aerosol processes. This approach allows the production of homogeneous nanoparticles with controlled size, shape, and structural properties [59–60].

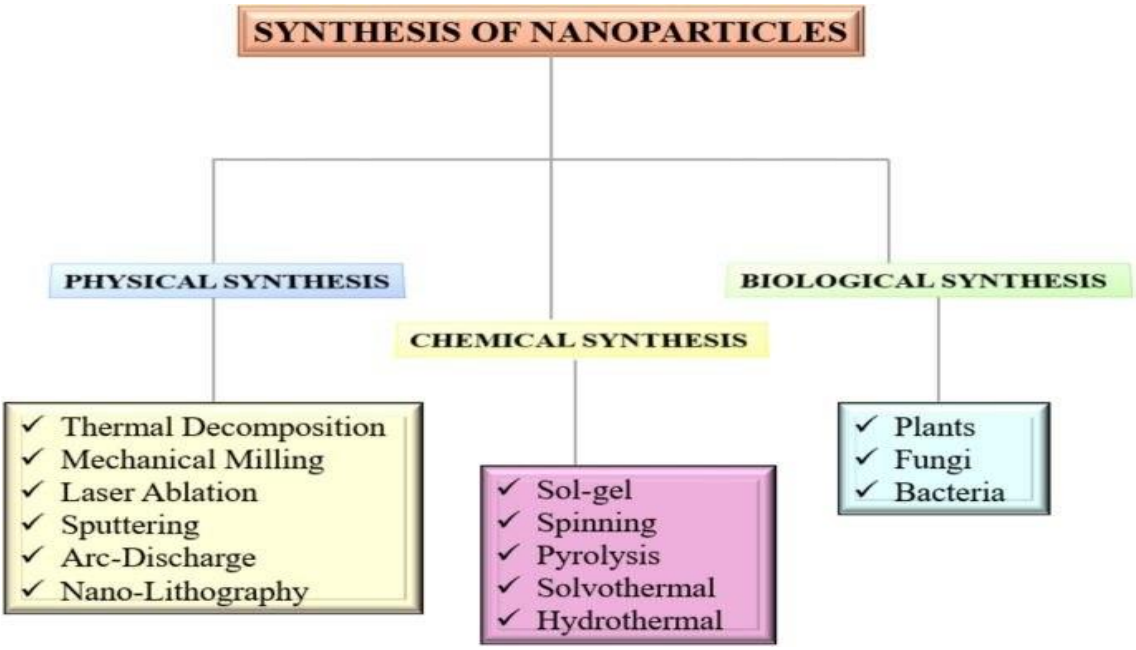


**Figure I- 6. Classification of nanoparticle synthesis techniques (Physical, Chemical, and Biological).**

### I.8.3. Green synthesis

The development of nanoparticle biosynthesis has significantly increased due to the economic limitations and environmental impacts of conventional methods. In this context, green synthesis represents a sustainable alternative based on the use of biological resources such as plant extracts and microorganisms. These biological systems provide natural compounds and biomolecules capable of mediating nanoparticle formation while reducing the need for toxic chemicals and minimizing environmental impact [61].

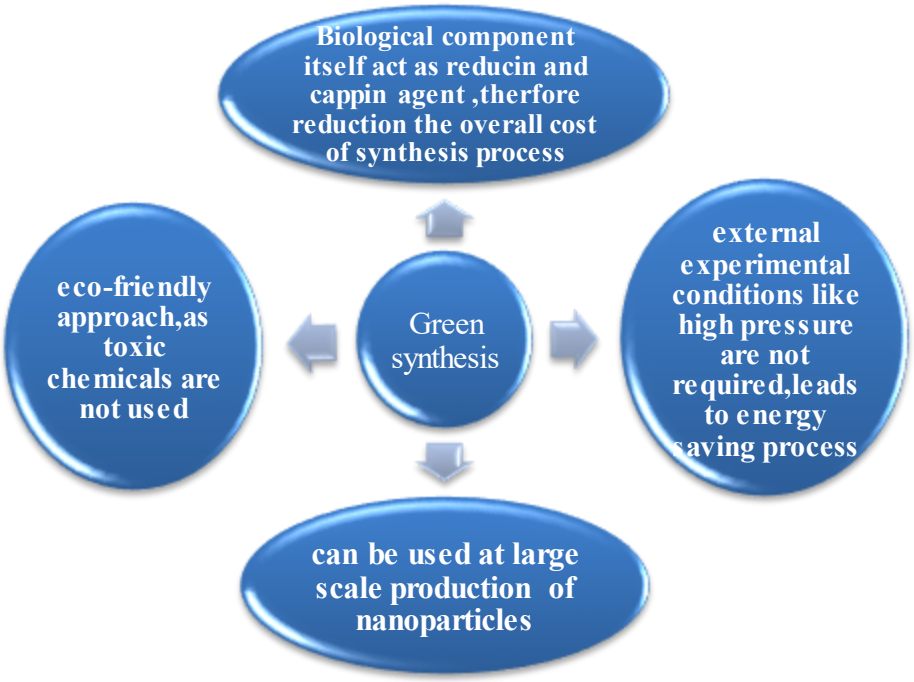


**Figure I- 7 Advantages and key benefits of green synthesis of nanoparticles.**

### I.8.3.1. Role of Phytochemicals in Green Synthesis

Plant extracts are rich in bioactive compounds such as polyphenols, flavonoids, terpenoids, tannins, and antioxidants. These phytochemicals play a crucial role in the green synthesis process by acting as reducing agents that convert iron ions into nanoparticles and as capping agents that stabilize the synthesized nanoparticles and prevent their aggregation. Furthermore, the nature and concentration of these compounds strongly influence the size, morphology, stability, and overall performance of the synthesized nanoparticles [62]

## I.9. Iron nano particles

Iron nanoparticles are nanoscale particles of iron with dimensions generally below 100 nm, characterized by high surface area, magnetic properties, and unique physicochemical characteristics that make them suitable for various environmental, biomedical, and industrial applications. [63].

### I.9.1. Types of iron nanoparticles

There are several types of iron nanoparticles, each with distinct chemical compositions and structural properties, as presented in **Table I- 5.**

**Table I- 5 Classification and characteristics of different iron-based nanoparticles**

| Type | Chemical formula | Mineral name | Description |
|---|---|---|---|
| **Zero-valent iron** | $Fe^0$ | Metallic iron | Iron in the zero-oxidation state with high reactivity and strong reducing properties.[64] |
| **Iron (II, III) oxide** | $Fe_3O_4$ | Magnetite | Mixed-valence iron oxide containing $Fe^{2+}$ and $Fe^{3+}$ with inverse spinel structure.[65] |
| **Iron (III) oxide** | $\alpha$-$Fe_2O_3$ | Hematite | Most stable iron oxide with rhombohedral crystal structure and $Fe^{3+}$ state.[65] |
| **Gamma-Iron (III) oxide** | $\gamma$-$Fe_2O$ | Maghemite | Oxidized form of magnetite containing mainly $Fe^{3+}$ ions.[65] |

### I.9.2Applications of iron nanoparticles

Iron nanoparticles exhibit several applications, among which:

#### I.9.2.1. Biomedical applications

Magnetic iron nanoparticles play an important role in biomedicine due to their remarkable magnetic properties [66]. They are used for therapeutic targeting, magnetic separation, and biological labeling, owing to their strong magnetization under an external magnetic field, which enables targeted drug delivery [67].

They are also used in magnetic resonance imaging (MRI) as contrast agents to improve the visualization of biological tissues, as well as in magnetic hyperthermia for the localized treatment of tumors [68].

### I.9.2.2. Environmental applications

In the context of environmental applications, iron nanoparticle technology has emerged as a promising material, particularly in advanced water and wastewater treatment. Owing to their high surface-to-volume ratio and strong chemical reactivity, these nanoparticles exhibit multifunctional behavior. In aquatic systems, they can act through coagulation effect [69]and adsorption processes. [70], contributing to the destabilization of colloidal particles and the removal of a wide range of contaminants.

Beyond these physicochemical interactions, iron nanoparticles also act as reactive agents capable of inducing the transformation and degradation of persistent organic pollutants, including chlorinated organic solvents [71], organochlorine pesticides, and synthetic dyes. Furthermore, they are effective in the removal of toxic heavy metal ions such as As(II), Pb(II), Cu(II), Ni(II), and Cr(VI). Recent studies also suggest a potential antimicrobial effect, attributed to the generation of reactive oxygen species (ROS), which may disrupt microbial cell structures. Overall, this versatility makes iron nanoparticles a promising approach for both industrial wastewater treatment and in situ groundwater remediation [72].

Moreover, iron-based nanoparticles can be considered as promising photocatalytic materials for water treatment; however, their direct application is often limited by issues such as particle aggregation and reduced accessibility of active surface sites. To overcome these limitations, activated carbon can be introduced as a supporting material due to its highly porous structure and large specific surface area. This not only enhances pollutant adsorption and concentrates contaminants near the catalytic sites, but also improves the dispersion of nanoparticles, leading to a synergistic effect between adsorption and photocatalytic degradation. [73]

# Chapter II: Materials and methods

This chapter outlines the experimental methods and protocols employed in the present study. It begins with the preparation of the aqueous extract of Cistus monspeliensis (CMLE) and the green synthesis of nanoparticles. The experimental setups and operating conditions for the coagulation–flocculation and photocatalytic degradation processes are then described in detail. Finally, the physicochemical characterization of the synthesized materials is presented using X-ray diffraction (DRX).

## I. 1 Study area:

For the purposes of this study, we used surface water samples collected from the Mexa Tarf station, as well as wastewater samples originating from the El Kala Wastewater Treatment Plant.

### I.1.1. The station of water treatment of Mexa

The station of water treatment of Mexa located in the northeastern part of Algeria, within the Wilaya of El Tarf, near the Algerian–Tunisian border. It belongs to a Mediterranean climatic region characterized by relatively high rainfall and the presence of important surface water resources, wetlands, and ecologically sensitive environments.

The study area comprises two main components: the Mexa Dam and the El Kala wastewater treatment plant (STEP), which together define the hydrological and environmental framework of the region.

The Mexa Dam is located in the commune of Bougous, approximately 75 km from El Tarf city and close to the Algerian–Tunisian border. It is part of the El Kebir East hydrological basin and drains a watershed area of about 579–650 $km^2$. Commissioned in 1998, the dam has a storage capacity of approximately 47 $hm^3$. It plays a key role in drinking water supply (AEP) for the cities of Annaba, El Tarf, and El Kala, as well as in supporting irrigation activities in surrounding agricultural areas.


**Figure II- 2. Mexa Dam area**

### I.1.2. STEP of El Kala

The El Kala wastewater treatment plant (STEP El Kala) was established in 1984 and covers an area of about 2 hectares. It is located approximately 1.5 km north-east of El Kala city, along the national road N44 leading to Oum Teboul. The plant is designed to treat approximately 1,900 $m^3$/day of municipal wastewater, collected through three pumping stations: Boulif, Mordjane, and Port stations, before being discharged into the natural receiving environment after treatment.

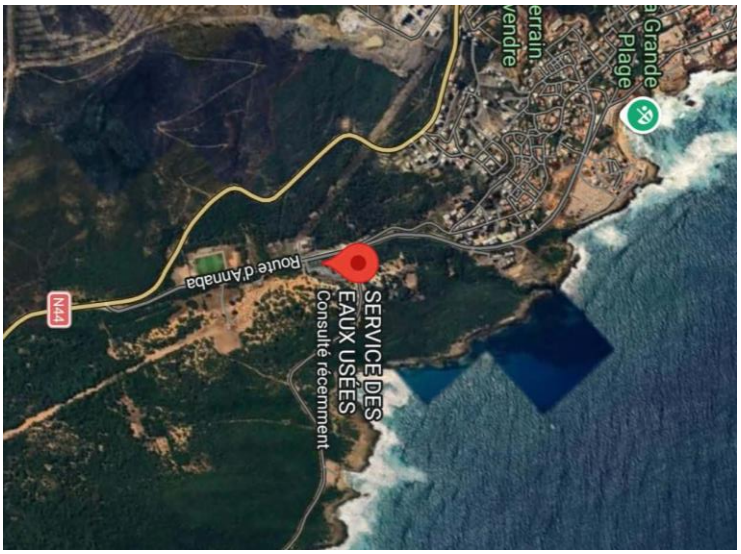


**Figure II- 3. STEP El Kala area**

Overall, the Mexa Dam and the STEP El Kala constitute the main components of the study area, illustrating the interaction between surface water resources, wastewater treatment infrastructure, and environmental protection in the region.

## I. 2. Preparation of the Plant Extract:

The leaves of (CM) were harvested and then washed with distilled water to remove dust and impurities. They were then dried in the shade at room temperature. Once completely dry, the leaves were ground to produce a fine, uniform powder. 10 g of this powder was placed in a Soxhlet extractor cartridge to obtain CMLE.

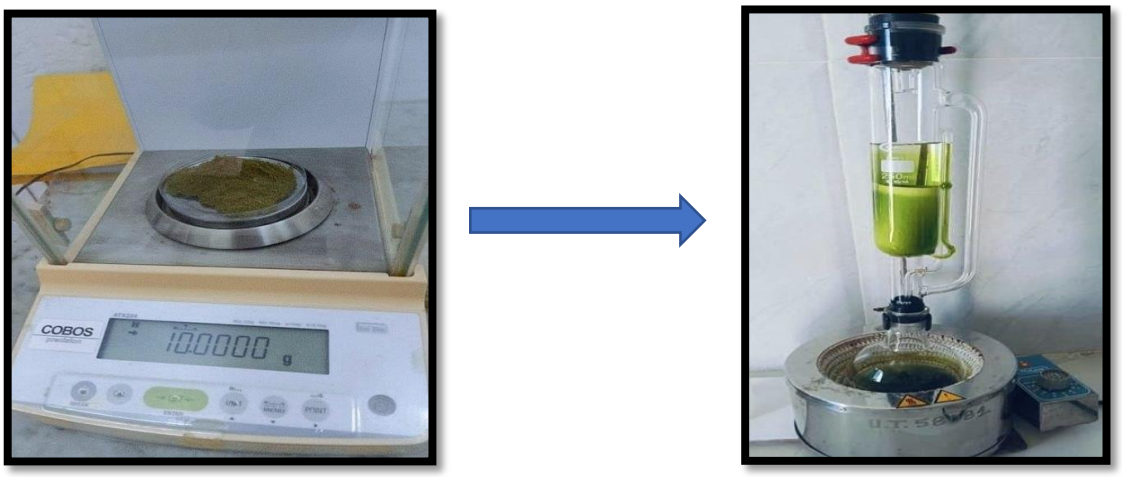


**Figure II- 4. Preparation of CMLE by soxhlet**

## I. 3. Green synthesis of iron oxide nanoparticles:

The iron oxide nanoparticles were synthesized via a green biosynthetic route using 50 mL of CMLE and a mixture of iron (III) chloride ($FeCl_3$) and iron (II) sulfate ($FeSO_4$). The reaction mixture was placed on a magnetic stirrer equipped with a heating plate and maintained at 60 °C under continuous stirring. Once the temperature had stabilized, a sodium hydroxide (NaOH) solution was added dropwise to adjust the pH to 11. The mixture was then kept under continuous stirring at 70 °C and 700 rpm for 3 h, allowing the formation of the iron oxide nanoparticles. At the end of the reaction, the mixture was left to settle, with nanoparticle precipitation mainly in the lower layer. The supernatant was carefully removed, and the remaining precipitate was collected and subjected to centrifugation. The nanoparticles were washed with methanol then distilled water and then dried in an oven for 24 hours. The nanoparticles were subjected to calcination in a furnace at elevated temperature for 2 hours.

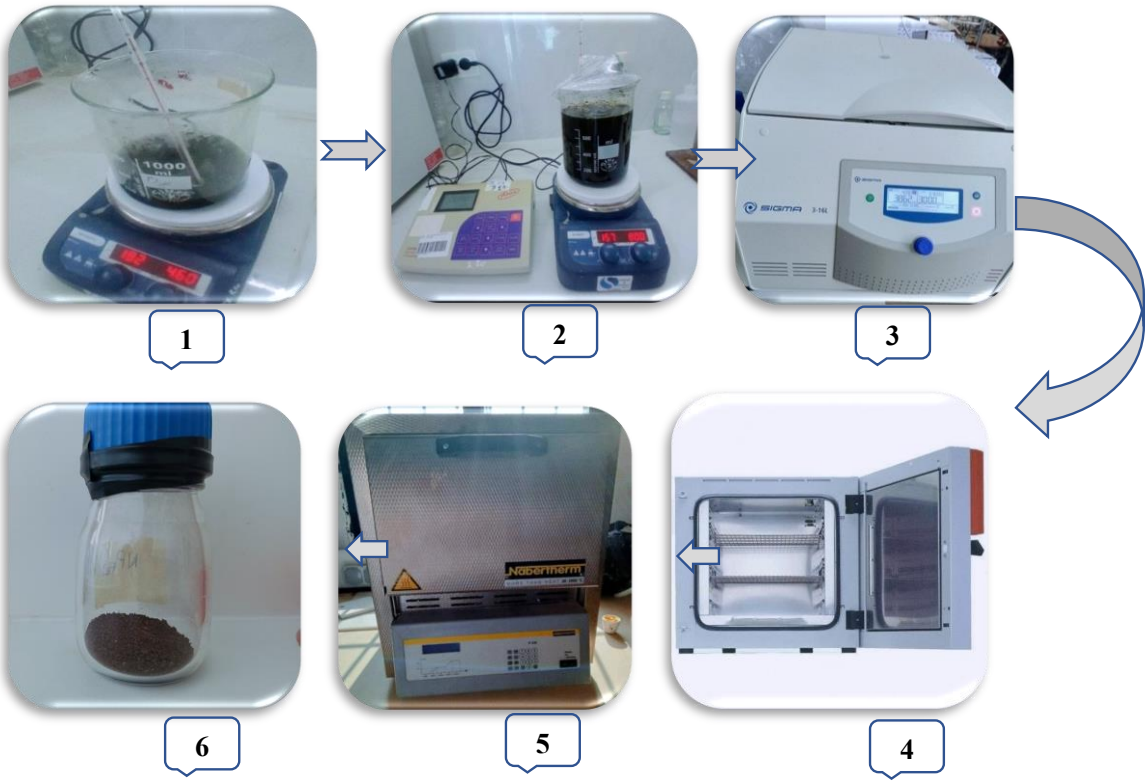


**Figure II- 5. Green synthesis of iron oxide nanoparticles**

## I.4. Characterization Techniques

### I.4.1. X-ray Diffraction

X-ray diffraction (XRD) is a structural analysis technique used to determine the crystal structure, phase and texture of materials.

In this study, the diffraction spectra of the nanoparticles were recorded using an X-ray diffractometer equipped with Cu $K_\alpha$ radiation ($\lambda$ = 1.5406 Å). Measurements were carried out over an angular range of $2\theta$ = 10° to 90°, in order to identify the crystalline phases present and estimate the average size of the crystallites.

## I.5.Water treatment process and water parameters:

### I.5.1. Protocol for determining the optimum dose of the bio-coagulant ($NP_{Fe}$) (jar test)

Equal volumes of surface water and wastewater (1 L each) were placed in beakers. Increasing amounts of $NP_{Fe}$ bio-coagulant (0.05; 0.25; 0.5; 1 and 3 g) were added to each sample. A very small dose of flocculant (0.05 mg/L) was added to promote floc formation and growth. The stirring blades were fitted and the mixture was agitated according to the following programme:

**Rapid stirring:** 150 rpm for 5 minutes**.**

**Slow stirring:** 40 rpm for 17 minutes**.**

At the end of agitation, the blades were raised carefully so as not to disturb the formed flocs. The samples were then left to stand for 30 minutes to allow the flocs to settle completely.

After settling, 0.5 L of supernatant was removed using a siphon from each beaker, as shown in the following figure

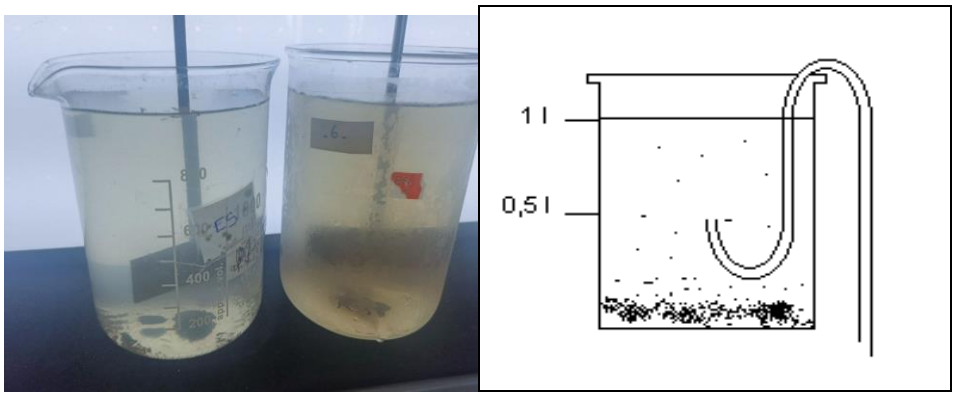


**Figure II- 6. Coagulation flocculation (jar test)**

### II.5.2. PH and Conductivity

pH and conductivity were measured with a Hach multi-parameter meter. The probes were first calibrated according to the manufacturer's instructions, then thoroughly rinsed with distilled water after each measurement to avoid cross-contamination


**Figure II- 7. Hach multi-parameter.**

### II.5.3. Turbidity

Turbidity of all samples was measured using a Hach turbidimeter. The instrument was calibrated prior to analysis and measurements were performed in triplicate to ensure accuracy and reproducibility.

**Figure II- 8. Hach turbidimeter.**

### II.5.4. Suspended Solids Measurement:

To determine the concentration of suspended solids (SS), we proceeded as follows: we took a 10 mL sample of homogeneous material and transferred it to a clean, dry cuvette, then placed it in the spectrophotometer. The SS concentration was read directly from the instrument.

**Figure II- 9. Suspended Solids Measurement.**

### II.5.5. Determination of Total Alkalinity (TA)

We took 100 mL of water for analysis using a graduated cylinder, then transferred it to a 250 mL Erlenmeyer flask. We added 2 to 3 drops of bromocresol green. The solution then turned blue (pH > 5.4). We filled the burette with 0.5 N sulphuric acid solution. We gently

swirled the Erlenmeyer flask and titrated the sample gradually with the sulphuric acid until the indicator changed color. The end point of the titration was reached when the color changed from blue to yellow-green. We recorded the volume (V) (in mL) of 0.5 N sulphuric acid used.

**Figure II- 10. TA Measurement.**

### II.5.6. Residual iron determination

In a 100 mL volumetric flask, introduce 50 mL of the sample and dilute if necessary. Add 1 mL of hydroxylamine hydrochloride, 2 mL of acetate buffer, and 2 mL of 1,10-phenanthroline. Shake the flask vigorously and leave it in the dark for 15 minutes. Measure the residual iron concentration at a wavelength of 510 nm.

**Figure II- 11. Residual iron Measurement**

### II.5.7. Determination of potassium permanganate oxidability – hot method in acid medium

#### II.5.7.1. Principle

The permanganate index of water is the mass concentration of oxygen equivalent to the quantity of permanganate ions consumed when a water sample is treated with permanganate under the specified conditions. The water sample is placed in the presence of a known quantity of potassium permanganate and sulphuric acid for a specified period (10 minutes). Part of the permanganate is reduced by the oxidizable matter in the sample. The excess permanganate is determined by adding an excess of oxalate, followed by titration of the excess oxalate with permanganate (back titration principle).

#### II.5.7.2. Procedure

We pour 100 ml of the water sample into an Erlenmeyer flask. We add 20 ml of concentrated sulphuric acid. We bring the mixture to the boil. We then add 20 ml of sodium oxalate until the solution has completely decolorized. Finally, we titrate the excess oxalate with a potassium permanganate solution until a pale pink color appears.

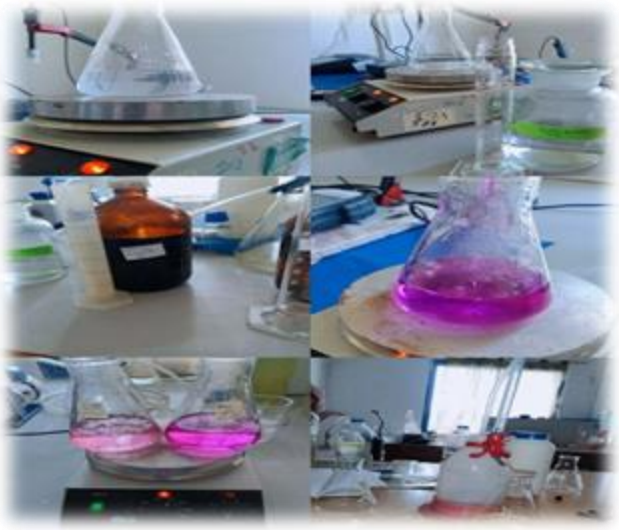

**Figure II- 12. potassium permanganate oxidability Measurement.**

### II.5.8. COD Measurement

Chemical oxygen demand (COD) was determined using a colorimetric method with commercial kits. We placed 10 ml of sample into a reaction tube, then added the reagent. The tubes were placed in a heating block at 150 °C for 2 hours. After returning to room temperature to allow the solution to stabilize, we measured the COD by spectrophotometry in direct measurement mode using the selected programmes.

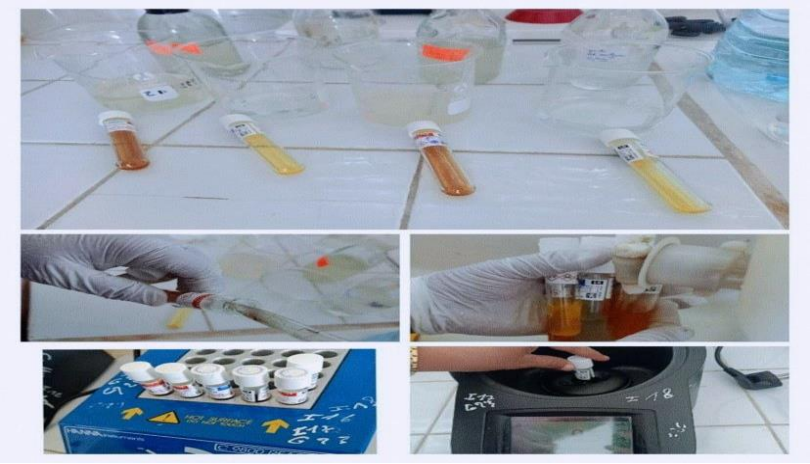

**Figure II- 13. COD Measurement.**

### II.5.9. $BOD_5$ Measurement

We took 95 ml of the water sample and transferred it to an amber glass bottle. We then placed a magnetic stir bar inside. After fitting the black rubber sleeve over the bottle neck, we used tweezers to insert the lithium hydroxide (LiOH) pellets inside the sleeve. Finally, we activated the sensor, then placed the assembly in a thermostatic incubator at 20 °C for five days, under gentle and continuous magnetic stirring.

**Figure II- 14. $DBO_5$ Measurement.**

### II. 5.10. Nitrite ($NO_2^-$) and nitrate ($NO_3^-$) Measurement

We measured the concentrations of nitrite and nitrate ions as follows: we took 10 ml of sample from each cuvette, then added the reagent. We then shook the cuvettes thoroughly and left them to stand for 20 minutes. Finally, using the spectrophotometer, we read the concentration directly.

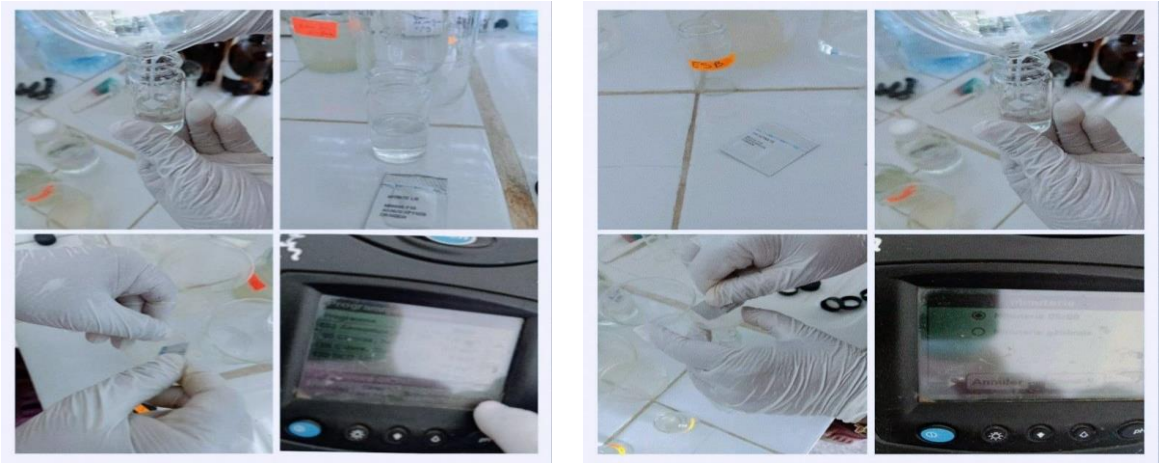

**Figure II- 15. Nitrite and Nitrate Measurement.**

### II.5.11. Phosphate ($PO_4^{3-}$) Measurement

We measured out 5.0 ml of the sample and transferred it to the reaction cuvette. We then mixed it thoroughly and left the mixture to stand for 10 minutes. Finally, we placed the cuvette in the spectrophotometer and recorded the phosphate concentration.

**Figure II- 16. Phosphate ($PO_4^{3-}$) Measurement.**

### II.5.12. Bacteriological analysis

As part of the assessment of the effectiveness of iron nanoparticles (FeNPs) used as a bio-coagulant, bacteriological analyses were carried out before and after treatment, in particular following the coagulation/flocculation and photocatalysis stages

### II.5.12.1. Testing for and quantifying total coliforms

We collect samples in sterile glass bottles or sterile single-use polyethylene vials. The detection and enumeration of total coliforms in water are carried out using the membrane filtration method. To do this, we filter 100 mL of water through a 0.45 µm filter membrane. The bacteria are thus retained on the membrane, which we then place on a selective culture medium (m-Endo agar). After incubation at 35 ± 0.5 °C for 24 ± 2 hours, we count the typical colonies (red colonies with a golden or green metallic sheen).

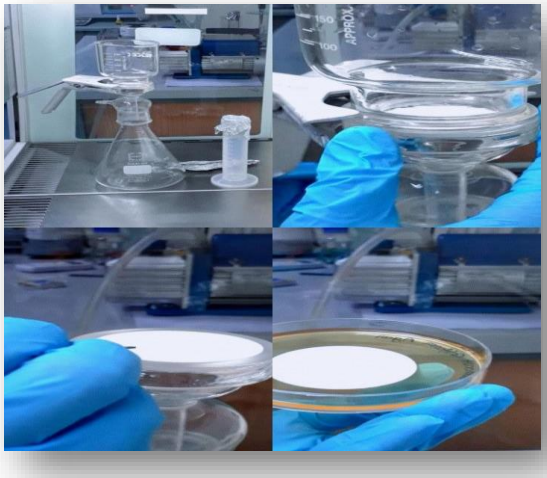

**Figure II- 17. Testing for and quantifying total coliforms.**

### II.5.12.2. Testing for and quantifying Faecal coliforms

Faecal coliforms have been used as microbiological indicators of faecal contamination in water. These bacteria constitute a subgroup of total coliforms, characterized by their ability to ferment lactose at a high temperature of 44.5 °C. The dominant species within this group is Escherichia coli (E. coli), which accounts for the vast majority of isolated strains.

For the detection and enumeration of these microorganisms, we opted for the membrane filtration method, a reference technique widely used in laboratories due to its quantitative nature, sensitivity and speed of execution.

The principle of this method is based on filtering a known volume of water sample through a sterile filter membrane with a pore size of 0.45 µm. The bacteria present are thus retained on the surface of the membrane. The membrane is then transferred to a selective culture

medium, usually m-FC agar, and incubated at 44.5 °C for 24 hours. After incubation, the typical colonies, which are blue to blue-violet in color, are counted. The results are finally expressed as CFU/100 ml (Colony-Forming Units per 100 milliliters).

### II.2.15.3. Detection and quantifying of spores of sulphite-reducing anaerobic bacteria membrane filtration method

Our objective is to detect and count sulphite-reducing anaerobic bacteria using membrane filtration. We follow this step with a culture on a selective medium, and then calculate their number in the sample. Before carrying out the test, we must heat the sample to be analyzed in a water bath at 75°C for 15 minutes, starting from the moment this temperature is reached.

We retained the bacterial spores on the 0.45 µm pore size filter after destroying the vegetative forms by heating the sample to 75°C for 15 minutes. We then incubated the membrane on Meat-Liver agar medium to which we added one ampoule of sodium sulphite and one ampoule of iron alum. Incubation lasted 48 hours at 37°C.

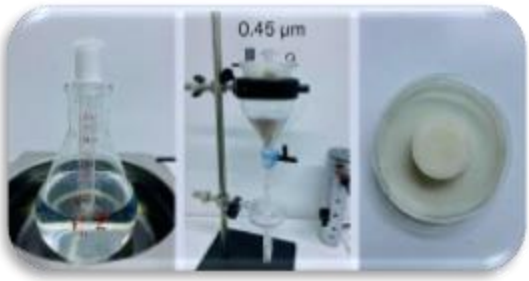


**Figure II- 18. Sulphite-reducing anaerobic bacteria detection test.**

## II.6. Photocatalysis

As part of our study, we used photocatalysis to enhance water clarification capacity. Our main objective was to evaluate the performance of residual iron nanoparticles present in the settled water following the jar test. To enhance photocatalytic efficiency, we incorporated increasing amounts of activated carbon (0.125, 0.25, 0.5 and 1 g/L) into our system, under UV irradiation, before proceeding to filtration.

Here is the experimental procedure we followed:

1. We weighed the activated carbon, then added it to the water and stirred the mixture to ensure good dispersion.
2. We then kept the mixture stirring in the dark for 30 minutes.
3. Subsequently, we exposed the suspension to UV light for one hour.
4. Immediately after irradiation, we filtered the suspension using a 77 µm syringe filter.

Following these steps, we measured various physico-chemical parameters of the treated water: turbidity, pH, conductivity, color and organic matter

**Figure II- 19. Photo of the experimental photocatalysis setup.**

# Chapter III: Results and Discussion

# III.1. Analysis and characterisation of Fe NPs biosynthesised from CMLE

## III.1.1. Analysis of X-ray diffraction spectra (XRD)

The **figure III- 1** shows the XRD pattern of Fe NPs produced by green synthesis from CMLE.

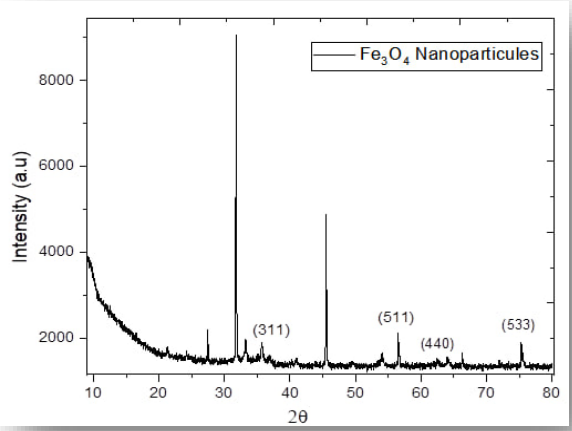


**Figure III- 2. X-ray diffractogram of $Fe_3O_4$ nanoparticles.**

The diffractogram matches perfectly with the structure of magnetite ($Fe_3O_4$), which has a cubic spinel structure. Here is a summary table of the main peaks visible on the diffractogram

**Table III- 1. Key diffraction peaks for Fe3O4 nanoparticles**

| 2θ (°) approx | Relative Intensity | (hkl) | Observation |
|---|---|---|---|
| **18.3** | Weak | (111) | Characteristic weak peak |
| **30.1** | Medium | (220) | Sharp peak |
| **35.5** | Very Strong | (311) | Most intense peak (dominant) |
| **37.1** | Weak | (222) | Shoulder or weak peak |
| **43.1** | Medium | (400) | Well visible |
| **53.5** | Weak | (422) | Weak peak |
| **57.0** | Strong | (511) | Prominent peak |
| **62.6** | Strong | (440) | Very characteristic peak |

| | | | |
|---|---|---|---|
| **71.0** | Weak | (620) | Weak peak |
| **74.0** | Medium | (533) | Visible peak on the right |

The peaks are sharp and relatively intense, indicating good crystallinity of the nanoparticles.

## III.2. Results of physico-chemical analyses of surface water and raw wastewater

In order to determine the optimal (necessary and sufficient) dose of our bio-coagulant, we carried out a detailed physico-chemical characterisation of the surface water and raw wastewater used in this study. These initial data provide a vital reference for interpreting the biocoagulant's mechanisms of action (charge neutralisation and adsorption) and for optimising our biocoagulant effectively.

The results of the physico-chemical analyses are presented in the following table

**Table III- 2. Physico-chemical analyses of surface water and raw wastewater.**

| Test | Surface water | Wastewater |
|---|---|---|
| **Turbidity (NTU)** | 156 | 27 |
| **PH** | 7,84 | 8,38 |
| **Conductivity (µs)** | 406 | 1164 |
| **iron concentration (mg/L)** | 0,22 | 0,5 |
| **Phosphate (mg/L)** | 4,88 | 5,61 |
| **Nitrite (mg/L)** | <0,01 | 0,025 |
| **Nitrate (mg/L)** | 2,9 | 4,5 |
| **COD (mg/L)** | 24 | 64 |
| **$BOD_5$ (mg/L)** | 9,5 | 33,5 |
| **Color** | 284 | 137 |
| **SS (mg/L)** | 288 | 35 |
| **Organic Matter (mg/L)** | 4,64 | 14.8 |
| **TAC (mg/L)** | 110 | 220 |

### III.2.1 Surface water

The surface water in the Mexa reservoir is characterised by high turbidity (156 NTU) and a high concentration of suspended solids (SS = 288 mg/L). This situation is mainly due to significant inputs of clay and sediment particles following heavy rainfall, a phenomenon exacerbated by the effects of climate change. Despite this high particulate load, the organic load remains low (COD = 24 mg/L and $BOD_5$ = 9.5 mg/L), indicating that the pollution is primarily of mineral and particulate origin rather than organic. The other parameters analysed (pH, conductivity, phosphates, nitrites, etc.) remain within acceptable limits for raw surface water, confirming that the pollution is predominantly of physical origin.

### III.2.2. wastewater

The raw wastewater has relatively low turbidity and suspended solids (SS) levels (27 NTU and 35 mg/L). This can be explained by the fact that the sampling point is located downstream of the oxygen injection (aeration) point, which already promotes some settling and oxidation of suspended matter. However, a relatively high colour value (137) is observed, indicating the presence of dissolved or colloidal organic compounds (humic substances or others). The organic load is moderate (COD = 64 mg/L and $BOD_5$ = 33.5 mg/L), corresponding to low to medium levels of organic pollution, typical of domestic wastewater that has already undergone partial pre-treatment. Furthermore, the high conductivity (1164 µS/cm) and TAC (220 mg/L) values are explained by high mineralisation and a significant concentration of dissolved ions. The alkaline pH (8.38) is also consistent with this profile

## III.3. Determining the optimum dose of the bio-coagulant (NPFe) (jar test)

### III.3.1. turbidity

After characterising the surface water and raw wastewater from a physico-chemical perspective, jar tests were carried out to assess coagulation-flocculation using the biocoagulant $NP_{Fe}$. The graph below shows the change in turbidity as a function of $NP_{Fe}$ concentration for both types of water.

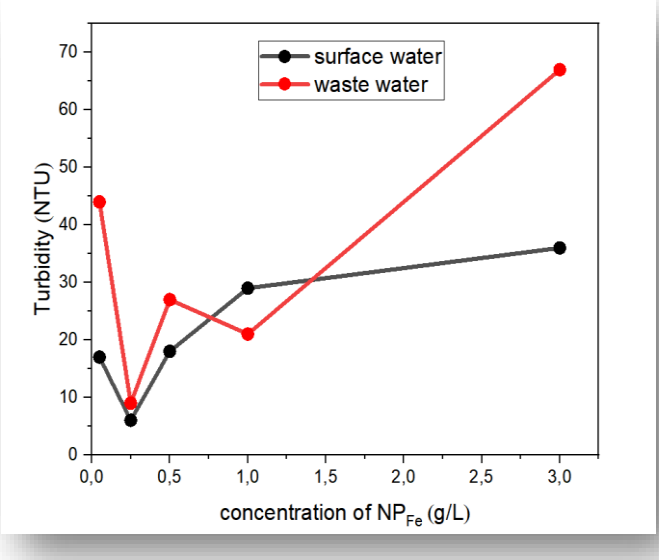


**Figure III- 3. turbidity as a function of $NP_{Fe}$ concentration.**

In Surface water the raw turbidity of the surface water is 156 NTU. From the very first dose tested (0.05 g/L of NP), turbidity drops dramatically to 17 NTU, a reduction of over 89%. The turbidity continues to increase slightly as the dose is increased, rising from 17 NTU to approximately 29 NTU at 1.0 g/L, and then to 36 NTU at 3.0 g/L.

The dose of 0.05 g/L is the optimal dose for surface water. It allows for excellent destabilisation of colloids and good sedimentation of suspended matter. Above this dose, an overdose is observed, leading to a slight re-increase in turbidity.

However, the raw turbidity of the wastewater is 24 NTU. At the first dose (0.05 g/L), an increase in turbidity is observed, rising to 44 NTU. From the second dose onwards, turbidity drops sharply to 9 NTU, corresponding to a very significant reduction (approximately 80% compared to the raw value). At intermediate doses (0.5–1.0 g/L), turbidity remains moderate (20–27 NTU), then rises sharply at high doses to reach 67 NTU at 3.0 g/L.

The optimum dose for raw wastewater is 0.25 g/L. Overdosing at high concentrations causes a marked destabilisation of the colloids.

### III.3.2. pH

The graph above shows how the pH of two types of water – surface water and wastewater – changes as a function of the concentration of added iron nanoparticles (FeNPs)

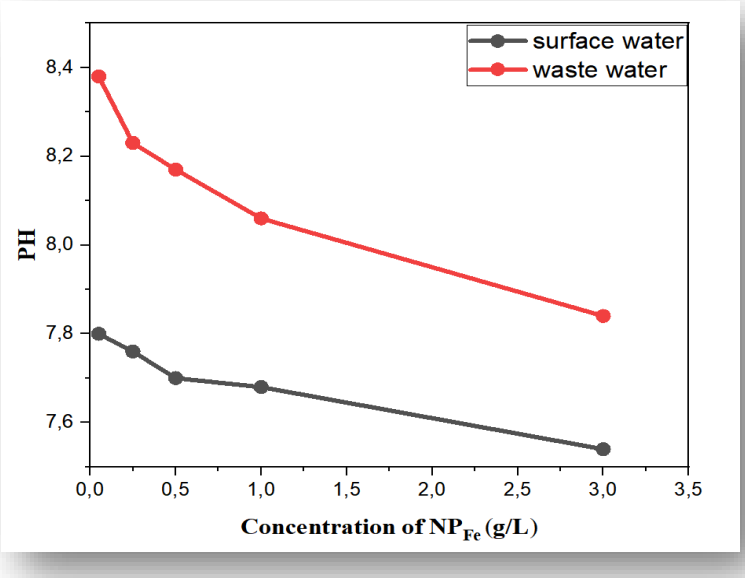


**Figure III- 4. pH as a function of $NP_{Fe}$ concentration.**

For surface water, the pH decreases steadily, falling from 7.8 to approximately 7.55. For wastewater, the addition of iron nanoparticles also leads to a decrease in pH, falling from 8.35 to 7.85; a gradual decrease in pH is observed. This indicates that the addition of iron nanoparticles has an acidifying effect on the medium.

### III.3.3. Conductivity

The graph above illustrates the change in electrical conductivity, expressed in µS, of two types of water – surface water and wastewater – as a function of the concentration of added iron nanoparticles (FeNPs).

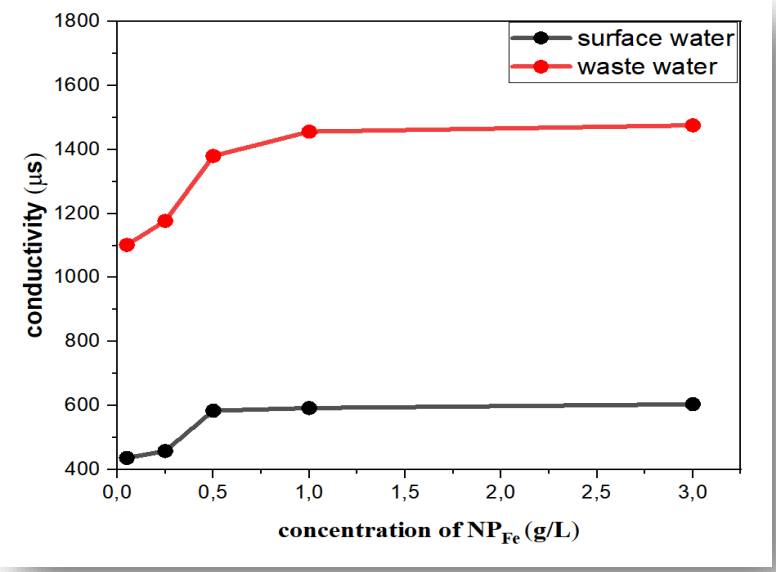


**Figure III- 5. Conductivity as a function of $NP_{Fe}$ concentration.**

With regard to surface water, we observe an average initial conductivity of approximately 406 µS. This value is characteristic of fresh water, which has a low concentration of dissolved salts. However, as soon as NPFe is added, the conductivity begins to rise significantly, reaching nearly 580 µS.In contrast, the wastewater has a significantly higher initial conductivity. This high conductivity is attributable to the presence of a greater quantity of dissolved matter, whether organic or inorganic, which is typical of wastewater. The introduction of NPFe into the wastewater also leads to a marked increase in conductivity, which can reach up to 1476 µS.

This increase in conductivity in both types of water, following the addition of NPFe and the coagulation-flocculation process, indicates the formation or release of ionic species in the medium. These dissolved ions, potentially resulting from the partial dissolution of NPFe or from chemical reactions involving the biocoagulant and NPFe, contribute to the overall increase in the ionic charge of the water samples.

### III.3.4. residual iron concentration

The graph above shows the trend in residual iron in surface water and wastewater as a function of the amount of NPFe added.

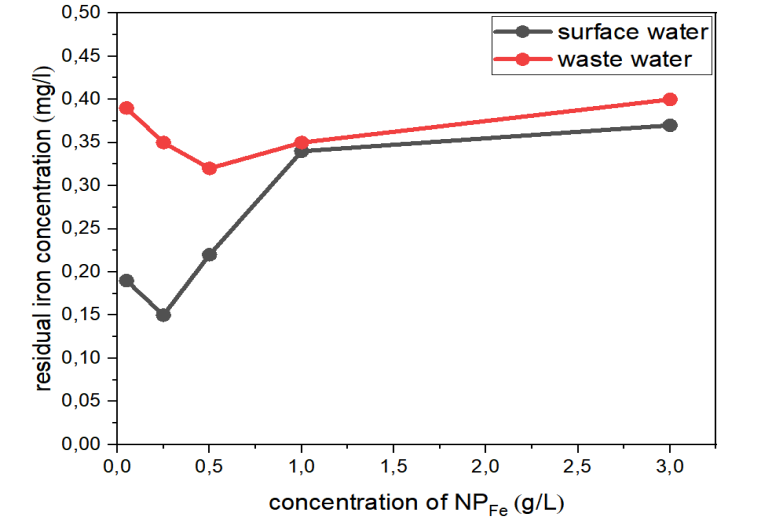


**Figure III- 6.residual iron as a function of NPFe concentration.**

For surface water, we observe that the initial residual iron concentration is approximately 0.22 mg/L. Upon addition of $NP_{Fe}$, this concentration decreases, reaching a minimum of approximately 0.15 mg/L at a dose of 0.25 g/L of $NP_{Fe}$. This point represents the optimal dose at which $NP_{Fe}$ acts effectively as a coagulant, promoting the removal of iron and other suspended particles. However, beyond this optimal concentration, the gradual increase in $NP_{Fe}$ leads to a marked rise in residual iron, reaching approximately 0.37 mg/L at a concentration of 3.0 g/L of $NP_{Fe}$. This increase indicates that an addition of $NP_{Fe}$ leads to an increase in iron concentration. With regard to wastewater, it has a significantly higher initial residual iron concentration of 0.5 mg/L. The addition of $NP_{Fe}$ also causes an initial decrease in residual iron, reaching a minimum of approximately 0.32 mg/L at an $NP_{Fe}$ concentration of approximately 0.5 g/L. This dosage proves to be the most effective for iron removal in wastewater. Similarly to surface water, increasing the $NP_{Fe}$ concentration beyond 0.5 g/L leads to a slight but steady increase in residual iron, reaching approximately 0.40 mg/L at the maximum concentration tested.

### III.3.5. Organic compounds

The graph above shows the change in residual organic matter concentration (expressed in mg/L) in surface water and wastewater as a function of the concentration of added iron nanoparticles (FeNPs)

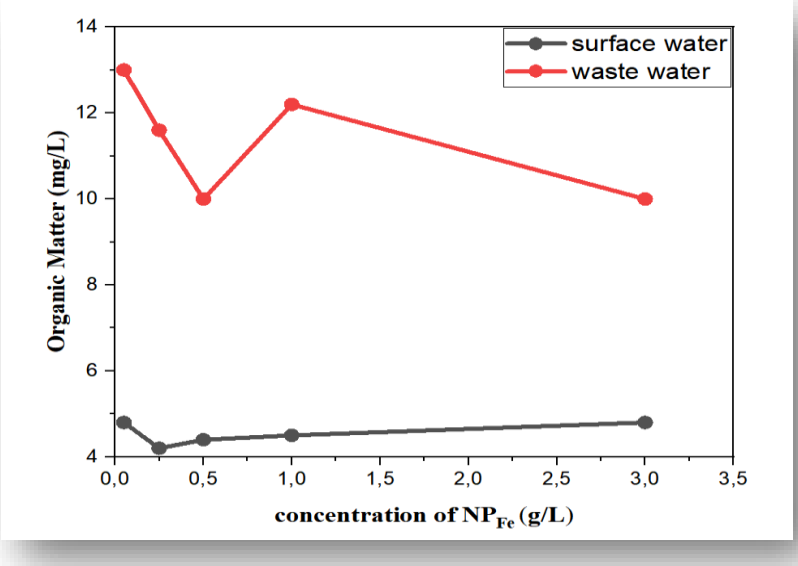


**Figure III- 7.Organic Matter as a function of $NP_{Fe}$ concentration.**

For surface water, with an initial organic matter concentration of 4.88 mg/L, we observe that upon addition of the first dose of $NP_{Fe}$ (0.05 g/L), the residual concentration decreases slightly to settle at around 4.7 mg/L. This reduction continues, with the minimum residual organic matter concentration being reached at approximately 4.2 mg/L for an $NP_{Fe}$ dose of 0.25 g/L. This value corresponds to the optimal $NP_{Fe}$ dose for surface water, demonstrating maximum removal efficiency at this point. Beyond this optimal concentration, the gradual increase in the amount of $NP_{Fe}$ leads to a slight but steady rise in residual organic matter, which reaches approximately 4.8 mg/L at a concentration of 3.0 g/L of $NP_{Fe}$. This suggests that an excessive dosage of $NP_{Fe}$ can lead to coagulant overload, potentially reducing its effectiveness. In contrast, for wastewater, where the initial organic matter concentration is significantly higher (14 mg/L), a substantial reduction is observed as soon as 0.05 g/L of $NP_{Fe}$ is added, with a residual concentration of approximately 12.8 mg/L. The concentration of residual organic matter continues to decrease, reaching a minimum of approximately 10 mg/L at an NPFe concentration of approximately 0.5 g/L. This dosage represents the point of maximum efficiency for the removal of organic matter from wastewater.

### III.3.6. Color

The graph above shows how the color of surface water and wastewater changes as a function of the concentration of added iron nanoparticles (FeNPs)

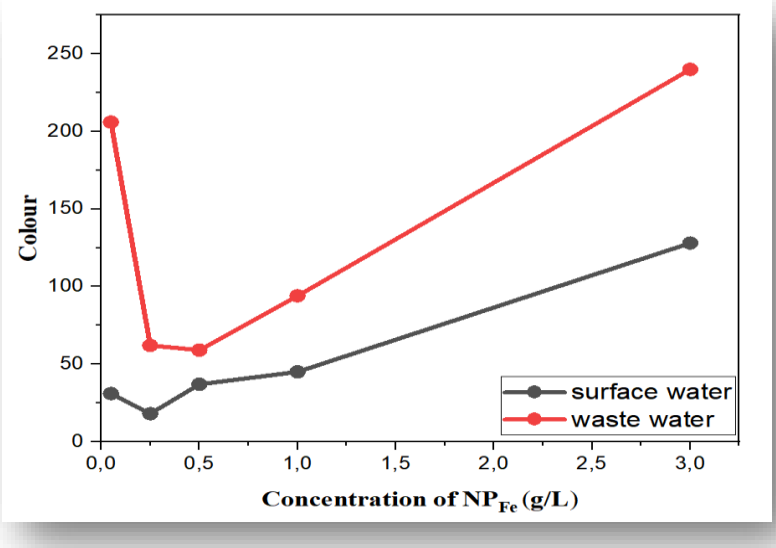


**Figure III- 8. Color as a function of $NP_{Fe}$ concentration.**

In surface water, where the initial colour was high, the addition of 0.05 g/L of $NP_{Fe}$ resulted in a reduction in colour, bringing it down to just 31. This observation demonstrates the exceptional decolourisation efficiency of $NP_{Fe}$ at low concentrations. The colour continued to decrease, reaching a minimum of 18 at an $NP_{Fe}$ concentration of 0.25 g/L. This value is identified as the optimal dose of $NP_{Fe}$ for the decolourisation of surface water under the experimental conditions applied. However, above 0.25 g/L, an increase in $NP_{Fe}$ concentration led to a gradual rise in colour, reaching 128 at 3.0 g/L of $NP_{Fe}$. This re-increase in colour is generally attributed to an overdose of the coagulant, and the appearance of colour linked to residual iron species. For the wastewater, which had an initial colour of 137, the addition of 0.05 g/L of $NP_{Fe}$ surprisingly led to an increase in colour, which rose to 206. Subsequently, the colour began to decrease, reaching a minimum of 59 at an $NP_{Fe}$ concentration of 0.5 g/L. This dosage represents the most effective dose for the decolourisation of the wastewater. Beyond this optimal concentration, a continuous increase in $NP_{Fe}$ led to a further significant rise in colour, reaching up to 240 units at 3.0 g/L of $NP_{Fe}$. This deterioration is also attributed to the excess coagulant, which disrupts the treatment's effectiveness at excessively high concentrations.

Based on these physicochemical parameters namely pH, conductivity, residual iron concentration, organic matter and colour, as determined by jar -testing. We confirm that a dose of 0.25 g/L of $NP_{Fe}$ represents the most effective solution. This concentration is therefore considered the optimal dose for the treatment of the two types of water studied.

## III.4. Photocatalytic Degradation Analysis

Following the coagulation-flocculation study, a series of photocatalysis experiments was conducted to investigate the material's potential for advanced oxidation. In this experimental section, we limited our investigation to the study of two operational variables: the amount of carbon used in the preparation or modification of the photocatalyst, and the contact time.

### III.4.1. Photocatalytic degradation in the absence and presence of activated carbon

The results comparing the efficacy of photocatalytic degradation alone with that of photocatalytic degradation assisted by activated carbon are shown in the following figures

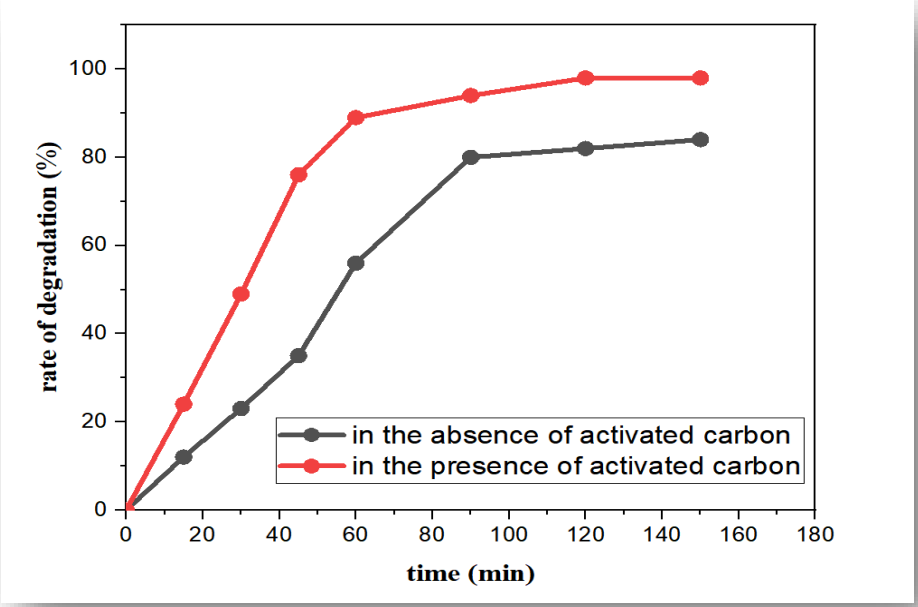


**Figure III- 9. Rate of photocatalytic degradation in the absence and presence of AC in surface water.**

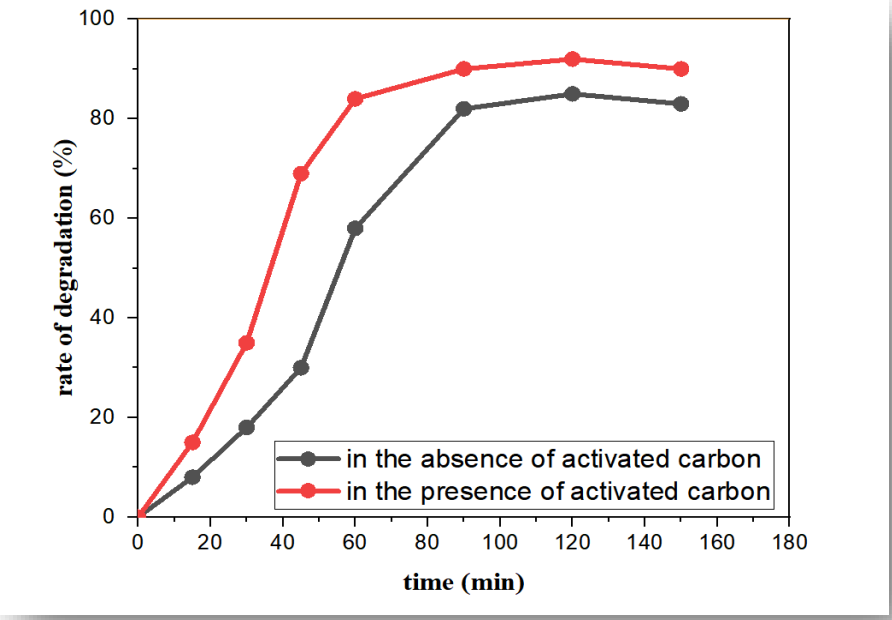


**Figure III- 10. Rate of photocatalytic degradation in the absence and presence of AC in wastewater.**

For surface water, we observe that the degradation of pollutants is gradual but relatively slow. After 60 minutes, the degradation rate reaches approximately 56%. The process slows down after 90 minutes, reaching approximately 80% at 100 minutes, then plateauing at around 83% after 120 minutes. The time required to reach maximum degradation is relatively long, but in the presence of activated carbon the kinetics improve. From the first 30 minutes onwards, the degradation rate is almost twice as high (around 49%) as in its absence (around 23%). The system achieves approximately 90% degradation in just 60 minutes, rising to nearly 98% after 120 minutes. for wastewater, in the absence of activated carbon, degradation in wastewater is also gradual. After 60 minutes, the degradation rate is approximately 58%. The process reaches a plateau of around 85% after 120 minutes, with a slight stabilisation. In the presence of activated carbon as with surface water, the presence of activated carbon accelerates and improves the degradation rate in wastewater. At 30 minutes, the degradation rate is approximately 35% with AC, compared to approximately 18% without AC. The process achieves a high degradation rate of approximately 83% within 60 minutes. The system stabilises at around 92% at 120 minutes, maintaining a rate higher than that of photocatalysis alone.

The addition of activated carbon creates a powerful synergy with photocatalysis, resulting in much faster degradation kinetics and a significantly higher final degradation rate in both surface water and wastewater.

### III.4.2. Dose of activated carbon

Following the optimisation of NPs, we sought to further improve the treatment performance for surface water and wastewater. With this in mind, we incorporated activated carbon adsorption into the process. This section is dedicated to studying the impact of different doses of activated carbon on water quality. We tested four specific concentrations of AC (0.125 g/L, 0.25 g/L, 0.5 g/L and 1 g/L) on samples of surface water and wastewater Each test was carried out in two distinct stages. First, the mixture was stirred continuously in the dark for 30 minutes. The suspension was then exposed to UV light for 1 hour. The treatment's effectiveness was assessed using physico-chemical parameters, namely: turbidity, pH, conductivity, total alkalinity (TAC), colour and organic matter. Our main objective is to characterise the contribution of activated carbon in this combined treatment system and to identify the optimal dose for achieving the best water quality.

#### III.4.2.1. Turbidity

This histogram shows how turbidity changes in surface water and wastewater as a function of the dose of activated carbon (AC) added.

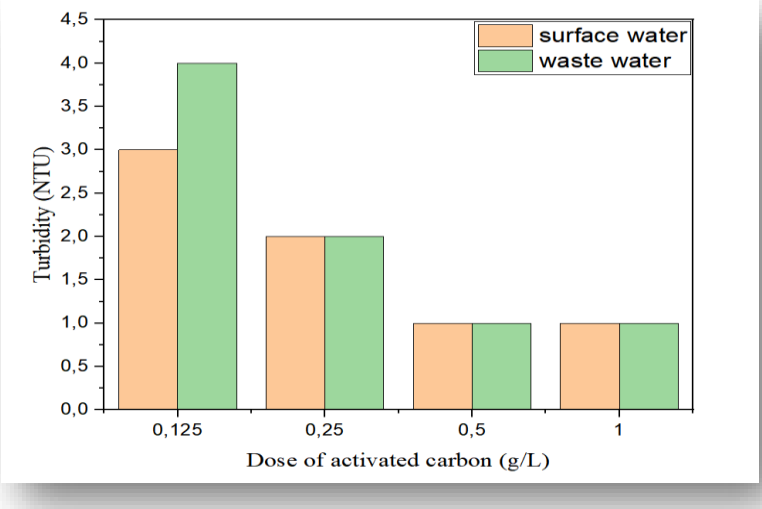


**Figure III- 11. turbidity as a function of AC concentration after photocatalysis experiment.**

For surface water with an initial turbidity of 6 NTU, the addition of activated carbon resulted in a gradual and significant reduction. From a dose of 0.5 g/L, turbidity reached a very low level of 1 NTU. It was found that, above this concentration of 0.5 g/L, increasing the dose of activated carbon did not result in any further improvement in terms of turbidity reduction. Similarly, wastewater, characterised by a higher initial turbidity of 9 NTU, also showed a significant reduction in turbidity. It reached a minimum of approximately 1 NTU at a dose of 0.5 g/L of activated carbon, confirming the effectiveness of this concentration for this type of water as well. Overall, activated carbon proved to be an extremely effective agent for reducing the turbidity of both types of water, despite their differences in initial load.

### III.4.2.2. pH

The graph shows how the pH of surface water and wastewater changes as a function of the dose of activated carbon (AC) added.

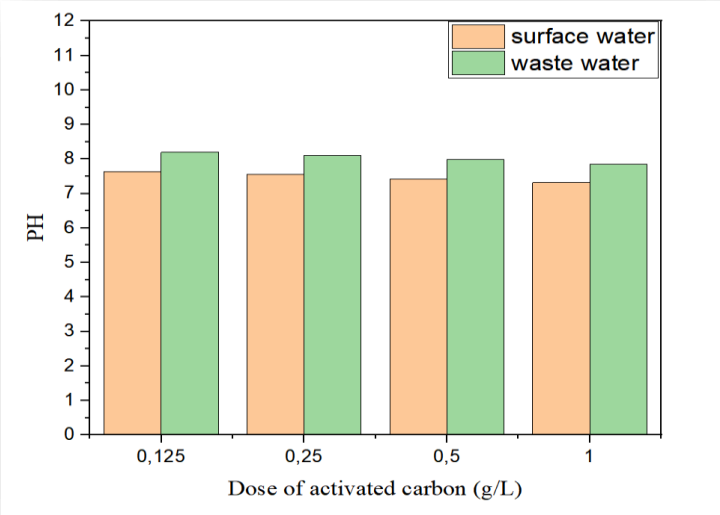


**Figure III- 12. pH as a function of AC concentration after photocatalysis experiment.**

For surface water, which had an initial pH of 7.76, the addition of activated carbon resulted in a slight decrease in pH, bringing it down to 7.36 across all the doses tested. Similarly, for wastewater, the initial pH of 8.23 also fell slightly to 7.85. Overall, it is important to note that the addition of activated carbon, despite this slight acidification, did not result in any major

changes in pH for either surface water or wastewater. The pH values are generally favourable and stable for water treatment.

### III.4.2.3. Conductivity

This graph shows the change in conductivity for surface water and wastewater as a function of the dose of activated carbon (AC) added during photocatalysis.

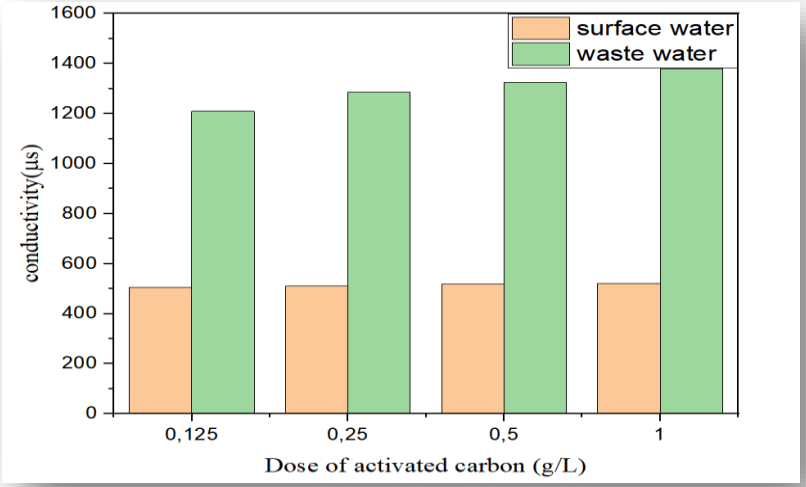


**Figure III- 13. conductivity as a function of AC concentration after photocatalysis experiment.**

This analysis shows that the addition of activated carbon leads to a slight increase in conductivity for both types of water. For surface water, conductivity rises from its initial value of 458 µS to a maximum of approximately 521 µS. Similarly, for wastewater, which has an initial conductivity of 1177 µS, conductivity increases to approximately 1380 µS.These variations, although observed, confirm that the addition of activated carbon does not significantly alter the overall conductivity of either surface water or wastewater, thereby maintaining the concentration of dissolved solids within an acceptable range and not compromising the overall quality of the treatment.

### III.4.2.4 TAC

This graph shows the variations in Total Alkalinity (TA) in surface water and wastewater, in relation to the different doses of activated carbon (AC) introduced

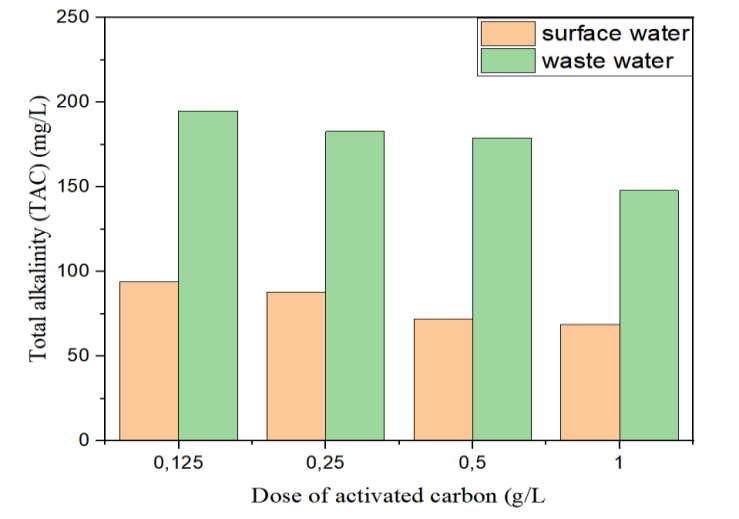


**Figure III- 14. TAC as a function of AC concentration after photocatalysis experiment.**

For surface water, which had an initial TAC of 108 mg/L, the addition of activated carbon led to a reduction in this value, eventually reaching 68 mg/L. Similarly, wastewater, which had an initial TAC of 202 mg/L, also showed a decrease in alkalinity, falling to 150 mg/L as the doses of activated carbon were increased.

### III.4.2.5. Organic compounds

This graph shows the change in organic matter concentration, expressed in mg/L, for surface water and wastewater, as a function of the different doses of activated carbon (AC) added.

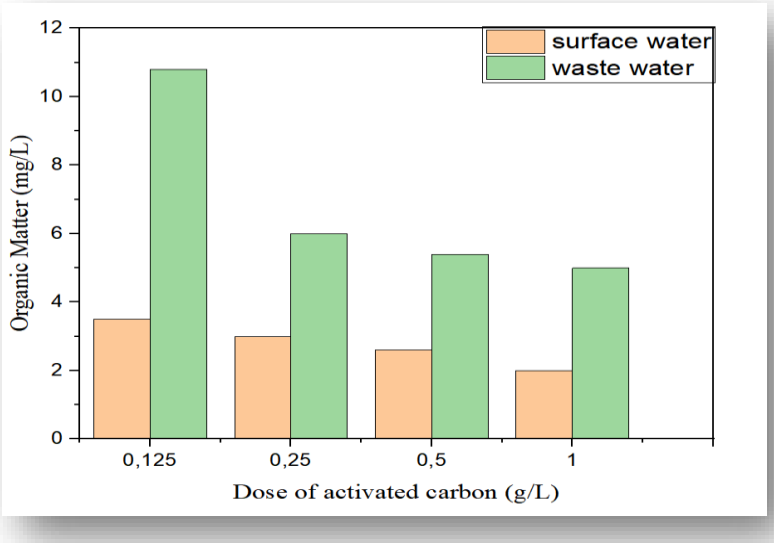


**Figure III- 15. Organic matter concentration as a function of AC concentration After photocatalysis experiment.**

Based on this analysis, we observe a significant reduction in the concentration of organic matter in both types of water, in proportion to the increase in the dose of activated carbon. This reduction is attributable to the combined action of adsorption by the activated carbon and photocatalytic degradation. For surface water, the concentration of organic matter, which stands at around 4.2 mg/L at a low dose of activated carbon, decreases gradually to reach around 2 mg/L. This residual concentration level meets drinking water quality standards, which are generally set at a value below 5 mg/L. As for wastewater, it also benefits from a significant reduction thanks to this combined treatment. Its organic matter concentration falls from around 12.8 mg/L to a final value of around 5 mg/L, demonstrating notable efficiency despite a higher initial pollutant load.

### III.4.2.6. Colour

This graph shows how the colour of surface water and wastewater changes in response to different doses of activated carbon (AC) added

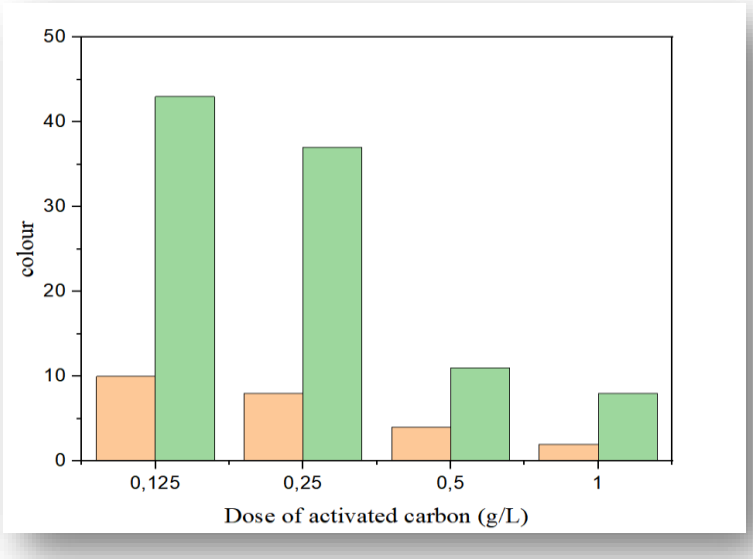


**Figure III- 16. colour as a function of AC concentration after photocatalysis experiment.**

This study highlights the remarkable effectiveness of activated carbon, acting in synergy with photocatalysis, in reducing colour in both types of water. For surface water, which had an initial colour of 18, the combined treatment achieved a reduction, lowering the colour to just 2. Wastewater, with an initial colour of 62, also underwent significant decolourisation, with its colour reduced to 8. These results confirm excellent decolourisation efficiency, highlighting the synergistic potential of activated carbon adsorption and photocatalysis to significantly improve water quality.

## III.5. Results of physico-chemical analyses of water following treatment

### III.5.1. Surface water

The table below shows the results of the physico-chemical analyses of surface water before and after the coagulation-flocculation treatment process and photocatalysis using activated carbon.

**Table III- 3. Results of the physico-chemical analyses of surface water before and after treatment.**

| Analysis | Surface water before treatment | Surface water after treatment |
|---|---|---|
| **Turbidity (NTU)** | 156 | 1 |
| **PH** | 7,84 | 7,43 |
| **Conductivity (µs)** | 406 | 518 |
| **iron concentration (mg/L)** | 0,22 | 0,09 |
| **Phosphate (mg/L)** | 4,88 | 0,69 |
| **Nitrite (mg/L)** | <0,01 | <0,01 |
| **Nitrate (mg/L)** | 2,9 | 1,2 |
| **COD (mg/L)** | 24 | 3 |
| **$BOD_5$ (mg/L)** | 9,5 | 1,4 |
| **Color** | 284 | 4 |
| **SS (mg/L)** | 288 | 4 |
| **Organic Matter (mg/L)** | 4,64 | 2 |
| **TA (mg/L)** | 110 | 72 |

### III.5.1.2. Interpretation of surface water results

A comparative analysis of the physico-chemical parameters of the surface water, before and after the combined treatment, reveals a highly significant improvement in water quality across all indicators.

**Turbidity** was reduced, falling from 156 NTU before treatment to an exceptionally low level of just 1 NTU afterwards. This performance demonstrates remarkably effective clarification, removing almost all suspended particles. The **pH** decreased slightly, from 7.84 to 7.43. This change keeps the pH within a near-neutral range, ensuring compatibility with most uses and ecosystems. As for **conductivity**, it increased slightly, rising from 406 µS to 518 µS. Although this increase suggests a slight release or production of ionic species (potentially due to coagulation), its magnitude remains moderate, indicating a limited impact on the overall concentration of dissolved solids. **The iron concentration** was significantly reduced, from 0.22 mg/L to 0.09 mg/L. This reduction is crucial for preventing issues with colour and metallic

taste, highlighting the effectiveness of the iron nanoparticle-based biocoagulant, followed by adsorption. We also note a very significant reduction in **phosphates**, from 4.88 mg/L to 0.69 mg/L, a result that is essential for preventing eutrophication of receiving water bodies. **The nitrite** concentration remained very low (<0.01 mg/L before and after treatment). Furthermore, **nitrate** levels were effectively reduced from 2.9 mg/L to 1.2 mg/L, which represents a positive improvement in overall water quality.

The indicators of organic pollution show particularly impressive results. The Chemical Oxygen Demand (**COD**) has been significantly reduced, falling from 24 mg/L to just 3 mg/L, indicating highly effective removal of oxidisable matter. Similarly, the 5-day Biochemical Oxygen Demand (**$BOD_5$**) showed a remarkable decrease, from 9.5 mg/L to a very low 1.4 mg/L. This value confirms that almost all biodegradable organic matter has been removed, a key indicator of very high-quality water. Colour was almost entirely eradicated, falling from 284 units to just 4 units, representing a remarkable aesthetic improvement and confirming the effective removal of chromophores. **Suspended solids** (SS) have been dramatically reduced, from 288 mg/L to 4 mg/L, which is directly linked to the effectiveness of coagulation-flocculation and clarification. Finally, the concentration of organic matter has decreased from 4.64 mg/L to 2 mg/L. This reduction is fully consistent with the improvements observed for COD, $BOD_5$ and colour, confirming the treatment's effectiveness on organic substances. The **TA** decreased from 110 mg/L to 72 mg/L. This reduction indicates a decrease in the water's buffering capacity, which could make it slightly more sensitive to future pH variations, but the values remain within a functional range.

### III.5.2. wastewater

The results of the physico-chemical analyses of the wastewater before and after coagulation-flocculation and photocatalysis treatment are presented in the table below.

**Table III- 4. Results of the physico-chemical analyses of wastewater before and after treatment.**

| Analysis | Wastewater before treatment | wastewater after treatment |
|---|---|---|
| **Turbidity (NTU)** | 27 | 1 |
| **PH** | 8,38 | 7,98 |
| **Conductivity (µs)** | 1164 | 1324 |
| **iron concentration (mg/L)** | 0,5 | 0,11 |
| **Phosphate (mg/L)** | 5,61 | 2,4 |
| **Nitrite (mg/L)** | 0,025 | 0,02 |
| **Nitrate (mg/L)** | 4,5 | 2,2 |
| **COD (mg/L)** | 64 | 7 |
| **$BOD_5$ (mg/L)** | 33,5 | 9 |
| **Color** | 137 | 11 |
| **SS (mg/L)** | 35 | 1 |
| **Organic Matter (mg/L)** | 14.8 | 5,4 |
| **TAC (mg/L)** | 220 | 179 |

**III.5.2.1Interpretation of wastewater results**

A comparative analysis of the physico-chemical parameters of the wastewater, before and after combined treatment, reveals an improvement in its quality across the majority of the indicators measured. **Turbidity** was reduced from 27 NTU before treatment to a very low level of 1 NTU afterwards. This improvement demonstrates extremely effective clarification, removing suspended particles. The **pH** decreased slightly, from 8.38 to 7.98. This moderate change keeps the pH within a range generally considered acceptable for the receiving environment. **Conductivity** increased significantly, rising from 1164 µS to 1324 µS. This increase suggests the release or production of ionic species during treatment, potentially linked to the coagulation process or the partial mineralisation of organic matter.

**The iron concentration** was significantly reduced, falling from 0.5 mg/L to 0.11 mg/L. This removal is essential for preventing problems with colour, taste and scaling, and demonstrates the effectiveness of the biocoagulant. **The phosphate** concentration showed only a reduction from 5.61 mg/L to 2.4 mg/L. This indicates that the combined treatment is not very effective at removing phosphates from wastewater. **Nitrite** concentrations, initially at 0.025 mg/L, decreased slightly to 0.02 mg/L. These levels remain very low and do not pose a

significant risk. However, **nitrate** levels were significantly reduced, falling from 4.5 mg/L to 2.2 mg/L, which represents a positive improvement in water quality. The indicators of organic pollution demonstrate remarkable performance. The **COD** was significantly reduced, falling from 64 mg/L to a very low 7 mg/L. This reduction demonstrates highly effective removal of oxidisable matter and organic pollutants. Similarly, the **$BOD_5$** showed a significant reduction, falling from 33.5 mg/L to 9 mg/L. Although this value remains higher than that obtained for surface water, it represents a substantial improvement for wastewater and indicates a high level of removal of biodegradable organic matter. A level of 9 mg/L may be considered acceptable according to specific discharge standards. **Color** has been significantly reduced, falling from 137 to just 11. This is a very significant improvement, and the concentration of **suspended solids** has been reduced from 35 mg/L to 1 mg/L, ensuring perfect clarification. The concentration of **organic matter** decreased from 14.8 mg/L to 5.4 mg/L. This reduction is fully consistent with the improvements observed for COD, $BOD_5$ and colour, confirming the treatment's effectiveness on the complex organic load of the wastewater. The TAC decreased from 220 mg/L to 179 mg/L. Although this reduction is smaller in percentage terms than for surface water, it indicates a decrease in the water's buffering capacity. However, the residual TAC remains at a high level, which gives the water good resistance to pH fluctuations.

## III.6. Results of bacteriological analyses

The table below shows the results of bacteriological analyses for surface water and wastewater at various stages of a coagulation-flocculation treatment process, and the final treatment following photocatalysis and activated carbon treatment

**Table III- 5. Results of the bacteriological analyses of surface and wastewater in various stages of treatment.**

| Test | SW before treatment | SW after coagulation-flocculation | SW after treatment | WW before Treatment | WW after coagulation-flocculation | WW after Treatment |
|---|---|---|---|---|---|---|
| **Total coliforms TC** | 16 | 10 | 5 | 28 | 21 | 15 |

| | | | | | | |
|---|---|---|---|---|---|---|
| **Faecal coliforms FC** | 0 | 0 | 0 | 2 | 1 | 0 |
| **Spores of sulphite-reducing anaerobic bacteria SRT** | 7 | 3 | 1 | 14 | 11 | 5 |

### III.6.1. Interpretation of the bacteriological results

Analysis of the results reveals a gradual and significant reduction in the bacterial load for both types of water, highlighting the effectiveness of the various treatment stages.

#### III.6.1.1. Surface water

**Total coliforms**: Initially, 16 units were present. After the coagulation-flocculation stage, this number was reduced to 10 units, demonstrating partial effectiveness in trapping bacteria within the flocs. The full treatment process further reduced these levels.

**Faecal coliforms**: The absence of faecal coliforms both before and after treatment (0 units) is a very positive health indicator, suggesting that the surface water was not contaminated with faecal matter and that the treatment maintained this absence.

**Spores of Anaerobic Sulphite-Reducing Bacteria**: The initial presence of 7 units of these spores, known for their resistance, was effectively reduced. After coagulation-flocculation, the number fell to 3, and the complete treatment reduced it to just 1 unit, confirming the very high efficacy of the process for these indicators of resistant contamination.

#### III.6.1.2. Wastewater

**Total Coliforms**: The wastewater showed high bacterial contamination, with 28 total coliform units prior to treatment. Coagulation-flocculation reduced this figure to 21, demonstrating initial effectiveness. Full treatment reduced the concentration to 15 units. Despite this significant reduction, total coliforms remain present in significant quantities.

**Faecal Coliforms:** The presence of 2 units prior to treatment indicated faecal contamination. Coagulation-flocculation reduced this figure to 1 unit. Full treatment resulted in total elimination, reaching 0 units. This result is particularly positive for improving the sanitary quality of the wastewater.

**Sulphite-Reducing Anaerobic Bacterial Spores**: Initially at 14 units, these spores were reduced to 11 following coagulation-flocculation. The full treatment resulted in a significant drop in concentration to 5, representing a notable reduction in these resistant organisms.

In general, the entire treatment process has demonstrated significant effectiveness in reducing the bacterial load for both types of water. The removal of faecal coliforms proved particularly effective, with these being completely eliminated (from 2 to 0 for wastewater), which is a very positive indicator of improved sanitary quality. The reduction in sulphite-reducing anaerobic bacterial spores is also notable in both cases, falling from 7 to 1 for surface water and from 14 to 5 for wastewater, which is encouraging given their resistance. However, it is important to note that, although reduced, total coliforms are not completely eliminated in either type of water. This persistence may require an additional final disinfection step to achieve levels compliant with the strictest standards

# General Conclusions

# General Conclusions

This thesis focused on the clarification and treatment of surface water and wastewater, exploring an integrated and innovative approach. We implemented a process combining the use of a biocoagulant derived from the biosynthesis of iron nanoparticles (NPFe), photocatalysis under UV irradiation, and adsorption on activated carbon. The main objective was to optimise the removal of major pollutants and significantly improve the overall quality of the treated water to meet environmental and health requirements.

In order to establish a solid foundation for our experimental approach and identify the most relevant treatment strategies, an in-depth literature review was conducted. This review enabled us to explore recent advances in water treatment techniques, notably the application of biocoagulants as sustainable alternatives to conventional chemical coagulants, the effectiveness of photocatalysis for the degradation of micropollutants and organic matter, as well as the crucial role of activated carbon in the adsorption of contaminants. This phase also highlighted the growing interest in combined processes aimed at capitalizing on the specific advantages of each method.

Our experimental methodology centered on jar tests rigorously conducted on surface water samples collected at the Mexa Tarf station and on wastewater from the El Kala Wastewater Treatment Plant (WWTP). Following preliminary optimization of the $NP_{Fe}$ dose for coagulation-flocculation, we investigated the impact of different doses of activated carbon on the pre-treated water, all under UV irradiation to activate the photocatalytic process. Performance was systematically assessed using a wide range of physico-chemical parameters – including turbidity, pH, conductivity, total alkalinity (TAC), colour, organic matter, COD, $BOD_5$, phosphates, nitrites, nitrates and iron – as well as through bacteriological analyses for total coliforms, faecal coliforms and spores of sulphite-reducing anaerobic bacteria.

The results obtained demonstrated the remarkable effectiveness of the combined treatment on both types of water. For surface water, a dramatic reduction in turbidity, color and suspended solids was observed. Indicators of organic pollution, such as COD, $BOD_5$ and organic matter, fell to levels compliant with drinking water standards. Wastewater also showed substantial improvements in turbidity, color, COD and $BOD_5$. Bacteriological analyses revealed the complete elimination of faecal coliforms in both types of water, as well as a significant reduction in total coliforms and spores. Despite minor and acceptable variations in pH,

conductivity and TAC, the overall quality of the treatment was not compromised. These findings confirm the promising potential of integrating biocoagulant biosynthesis, $NP_{Fe}$, photocatalysis and activated carbon to produce high-quality water from various sources.

# References

[1] European Environment Agency (EEA) (2023). Europe's environment: Water quality and pressures on aquatic ecosystems.

[2] U.S. Environmental Protection Agency (EPA) (2023). Drinking Water Contaminant Regulation and Treatment Technologies Report.

[3] Frontiers in Environmental Science (2024). Review on advanced oxidation processes and photocatalysis for wastewater treatment applications.

[4] Materials Today Nano (2023). Nanomaterials for environmental remediation and water purification: mechanisms and applications.

[5] Journal of Cleaner Production (2024). Advanced oxidation and hybrid technologies for sustainable wastewater treatment: a critical review.

[6] Nature Reviews Materials (2022). Semiconductor photocatalysis and engineered nanomaterials for environmental applications

[7] Singh, V. (2024). Water pollution. In Textbook of Environment and Ecology (pp. 253–266). Springer.

[8] Ali, S. (2022). About half of US water 'too polluted' for swimming, fishing or drinking, report finds. The Hill.

[9] Chapman, D. (Ed.). (1992). Water Quality Assessments: A Guide to the Use of Biota, Sediments and Water in Environmental Monitoring. London: Chapman & Hall, on behalf of UNESCO, WHO and UNEP.

[10] Belghiti, M. L., CHAHLAOUI, A., Bengoumi, D., & El Moustaine, R. (2013). Etude de la qualité physico- chimique et bactériologique des eaux souterraines de la nappe plio-quaternaire dans la région de Meknès (Maroc). LARHYSS Journal P-ISSN 1112-3680/E-ISSN 2521-9782, (14).

[11] Abboudi A, Tabyaoui H, El Hamichi F. (2014), Etude de la qualité physico-chimique et contamination métallique des eaux de surface du bassin versant de guigou, maroc , European Scientific Journal, n° 23,( aout 2014) , p 84 -94.

[12] Mahe, A., Salihu, N., & Sani, M. M. (2024). Perspective chapter: Physicochemical Parameters and Water Quality. In Sustaining Water Quality.

[13] MERABET. S, 2010. Évaluation de la qualité physico-chimique des eaux brutes et Distribuées du barrage réservoir de beni Haroun. Mémoire de magister chimie analytique. Université mentouri de Constantine. pp 4, 5,9

[14] Misman, N. A., Sharif, M. F., Chowdhury, A. J. K., & Azizan, N. H. (2023). Water pollution and the assessment of water quality parameters: A review. Desalination and Water Treatment,

[15] Chaoui. M., (2013). Contribution a l'étude de la qualité physico-chimique et métallique des eaux de surface (oued Moulouya/barrage Hassan II) au voisinage de la mine abandonnée Zeïda (haute Moulouya). Mémoire de Master. Université cadi ayyad.13p.

[16] Martin, A. (1982). *L'analyse de l'eau : méthodes et techniques*. Paris: La Documentation Française

[17] Satin, M., & Selmi, N. (1999*). Mémoire de fin d'études sur l'analyse et l'évaluation de la qualité des eaux*

[18] Bourgeois, C. M., Mescle, J. F., & Zucca, J. (1991). Microbiologie alimentaire : Aspect microbiologique de la *sécurité et de la qualité des aliments* (Vol. 1). Paris : Éditions Tec & Doc

[19] La Rodier, J., Bazin, C., Broutin, J. P., Chambon, P., Champsaur, H., & Rodi, L. (2005). L'analyse de l'eau : Eaux naturelles, eaux résiduaires, eau de mer (8e éd.). Paris : Dunodvoisier.

[20] Rodier, J., Legube, B., & Merlet, N. (2009). L'analyse de l'eau : Eaux naturelles, eaux résiduaires, eau de mer (9e éd.). Paris : Dunod

[21] Agbota, Y. (2017). Inactivation de la bactérie Escherichia coli dans l'eau par le jus de citron (Article, École de technologie supérieure, Université du Québec)

[22] Edwards, T. M., Puglis, H. J., Kent, D. B., Durán, J. L., Bradshaw, L. M., & Farag, A. M. (2024). Ammonia and aquatic ecosystems–A review of global sources, biogeochemical cycling, and effects on fish. *Science of The Total Environment*, *907*, 167911.

[23] Botté, A., Zaidi, M., Guery, J., Fichet, D., & Leignel, V. (2022). Aluminium in aquatic environments: abundance and ecotoxicological impacts. *Aquatic Ecology*, *56*(3), 751-773.

[24] O. El hani, A. Karrat, K. Digua, and A. Amine, "Development of a simplified spectrophotometric method for nitrite determination in water samples," Spectrochim. Acta A Mol. Biomol. Spectrosc., vol. 267, p. 120574, Feb. 2022, doi: 10.1016/J.SAA.2021.120574.

[25] Liu, Y., Zhang, Y., Lv, H., Zhao, L., Wang, X., Yang, Z., ... & Gu, H. (2025). Research on the traceability and treatment of nitrate pollution in groundwater: a comprehensive review. *Environmental Geochemistry and Health*, *47*(4), 107.

[26] Jiang, X., Su, S., Ren, B., Qiu, Y., Wang, S., & Yang, X. (2025). Lanthanum-Doped iron MOFs: A sustainable solution for Arsenic (V) and phosphate pollution in water. *Separation and Purification Technology*, *354*, 129098.

[27] Ben Mansour, H., Boughzala, O., Dridi, D., Barillier, D., Chekir-Ghedira, L., & Mosrati, R. (2011). Les colorants textiles sources de contamination de l'eau : Criblage de la toxicité et des méthodes de traitement. Revue des sciences de l'eau / Journal of Water Science, 24(3), 209–238.

[28] Parsons, S. A., & Jefferson, B. (2006). *Introduction to potable water treatment processes* (Vol. 5). Hoboken, NJ, USA: Blackwell Pub..

[29] Lucas, M. S., Teixeira, A. R., Jorge, N., & Peres, J. A. (2025). Industrial wastewater treatment by coagulation–flocculation and advanced oxidation processes: A review. *Water*, *17*(13), 1934.

[30] M. S. Lucas, A. R. Teixeira, N. Jorge, and J. A. Peres, "Industrial Wastewater Treatment by Coagulation–Flocculation and Advanced Oxidation Processes: A Review," Water 2025, Vol. 17, Page 1934, vol. 17, no. 13, p. 1934, Jun. 2025, doi: 10.3390/W17131934.

[31] Bartlett, S., Gladman, D., Lacaille, N. J. D., & Westby, M. (2024). Le Journal de la Société canadienne de rhumatologie.

[32] EzzianeS., 2007 : Traitement des eaux de rejets de l'unité CERAMIT « TENES », Mémoire de Magister, Département de génie des procédés, Faculté des sciences et sciences de l'ingénieur ; Université Hassiba Ben Bouali, Chlef. http://www.ing-dz.com.

[33] Boursali I Etude expérimentale de la coagulation-floculation par le sulfate Ferrique et le chlorure ferrique des matières en suspension. Mémoire d'ingénieur d'états en géologie. Université Abou BakrBalkaid. Tlemcen. (2011)

[34] VALENTIN.N., 2000 : « Construction d'un capteur logiciel pour le contrôle automatique du procédé de coagulation en traitement d'eau potable ». Thèse de Doctorat, UTC, Lyonnaise des Eaux ,CNRS.

**[35]** Attia, M. S., Abdel-Wahed, M. S., Algethami, F. K., & El-Kalliny, A. S. (2026). Advanced oxidation processes (AOPs) for drinking water treatment: A state-of-the-art review on applications, efficacy, and implementation challenges. RSC Advances, 16, 22186–22203.

[36] Andreozzi, R., Caprio, V., Insola, A., & Marotta, R. (1999). Advanced oxidation processes (AOP) for water purification and recovery. *Catalysis Today, 53*(1), 51–59

[37] T. Liu *et al.*, "Synergistic Effect of Charge Separation and Multiple Reactive Oxygen Species Generation on Boosting Photocatalytic Degradation of Fluvastatin by ZnIn2S4/Bi2WO6 Z-Scheme Heterostructured Photocatalytst," *Toxics*, vol. 10, no. 10, p. 555, Oct. 2022, doi: 10.3390/TOXICS10100555/S1.

[38] Zaviska, F., Drogui, P., Mercier, G., & Blais, J. (2009). Procédés d'oxydation avancée dans le traitement des eaux et des effluents industriels : Application à la dégradation des polluants réfractaires. Revue des sciences de l'eau / Journal of Water Science, 22(4), 535–564

[39] H. Y. Ma, L. Zhao, L. H. Guo, H. Zhang, F. J. Chen, and W. C. Yu, "Roles of reactive oxygen species (ROS) in the photocatalytic degradation of pentachlorophenol and its main toxic intermediates by TiO2/UV," *J Hazard Mater*, vol. 369, pp. 719–726, May 2019.

[40] Ibhadon, A. O., & Fitzpatrick, P. (2013). Heterogeneous photocatalysis: recent advances and applications. *Catalysts*, *3*(1), 189-218.

[41] Morshedy, A. S., El-Fawal, E. M., Zaki, T., El-Zahhar, A. A., Alghamdi, M. M., & El Naggar, A. M. (2024). A review on heterogeneous photocatalytic materials: Mechanism, perspectives, and environmental and energy sustainability applications. *Inorganic Chemistry Communications*, *163*, 112307

[42] Chakravorty, A.; Roy, S. A review of photocatalysis, basic principles, processes, and materials. Sustain. Chem. Environ. **2024**, 8, 100155.

[43] Parida, V.K.; Srivastava, S.K.; Gupta, A.K.; Rawat, A. A review on nanomaterial-based heterogeneous photocatalysts for removal of contaminants from water. Mater. Express 2023, 13, 1–28.

[44] Etacheri, V., Di Valentin, C., Schneider, J., Bahnemann, D., & Pillai, S. C. (2015). Visible-light activation of $TiO_2$ photocatalysts: Advances in theory and experiments. Journal of Photochemistry and Photobiology C: Photochemistry Reviews, 25, 1–29

[45] Diallo, I., Thiam, A., Diop, B., Mbow, B., Fofana, M., Faye, F. D., ... & Sene, A. (2025). Brief review on the evolution of catalysis in chemistry. *American Journal of Chemistry*, 25-42.

[46] Sultana, J., Noureen, S., Rani, M., Ahmad, I., Wang, C., Li, C., ... & Waseem, A. (2025). Visible-light-driven perovskite carbonaceous photocatalyst using LaNiO3/rGO composite for environmental remediation. *Catalysis Today*, *451*, 115238.

[47] S. Samia, Dégradation d'un colorant cationique par photocatalyse, électro oxydation et leur couplage, thèse de doctorat, 2018, Université Badji Mokhtar-Annaba, Algérie.

[48] Lê Vinh.H , Comparaison des rendements énergétiques de dégradation de trois composés organiques par plusieurs procédés d9oxydation avancés en milieu aqueux, thèse de doctorat , L9UNIVERSITE DE POITIERS,2009

[49] Chong, M. N., Jin, B., Chow, C. W. K., & Saint, C. (2010). Recent developments in photocatalytic water treatment technology: A review. Water Research, 44(10), 2997–3027.

[50] Malato, S., Fernández-Ibáñez, P., Maldonado, M. I., Blanco, J., & Gernjak, W. (2009). Decontamination and disinfection of water by solar photocatalysis: Recent overview and trends. Catalysis Today, 147(1), 1–59.

[51] Hoffmann, M. R., Martin, S. T., Choi, W., & Bahnemann, D. W. (1995). Environmental applications of semiconductor photocatalysis. Chemical Reviews, 95(1), 69–96.

[52] A. A. Ayachi, "Synthesis of metal oxide nanoparticles for solar photocatalytic applications," 2015.

[53] W. Bekhti, "Hydrothermal synthesis and characterization of zinc oxide micro/nanostructures," Lyon 1, 2015.

**[54]** D.E. Belfennache, Elaboration et étude de nanoparticules Au/TiO2 et Ag/TiO2, Thèse de Doctorat, Département De Physique, Université MENTOURI, Constantine, 2012, pp.5-6.

[55] D.E. Belfennache, Elaboration and study of Au/TiO2 and Ag/TiO2 nanoparticles, PhD thesis, Department of Physics, MENTOURI University, Constantine, 2012, pp.5-6.

[56] Dheyab MA, Aziz AA, Jameel MS, Noqta OA, Khaniabadi PM, Mehrdel B. Synthesis and coating methods of biocompatible iron oxide/gold nanoparticle and nanocomposite for biomedical applications. Chin J Phys. 2020;64:305–25.

[57] Choi WI, Kim J-Y, Heo SU, Jeong YY, Kim YH, Tae G. The effect of mechanical properties of iron oxide nanoparticle-loaded functional nano-carrier on tumour targeting and imaging. J Control Release. 2012;162(2):267–75.

[58] Seabra AB, Pelegrino MT, Haddad PS. Antimicrobial applications of superparamagnetic iron oxide nanoparticles. Nanostruct Antimicrob Ther. 2017.

[59] 58Andrade RGD, Veloso SRS, Castanheira EMS. Shape anisotropic iron oxide-based magnetic nanoparticles: synthesis and biomedical applications. Int J Mol Sci. 2020;21(7):2455.

[60] Friedrich RP, Cicha I, Alexiou C. Iron oxide nanoparticles in regenerative and tissue engineering. Nanomaterials. 2021;11:2337.

[61] Singh, J., Dutta, T., Kim, K.-H., Rawat, M., Samddar, P., & Kumar, P. (2018). 'Green' synthesis of metals and their oxide nanoparticles: Applications for environmental remediation. Journal of Nanobiotechnology, 16(1), 84.

[62] Saif, S., Tahir, A., & Chen, Y. (2016). Green synthesis of iron nanoparticles and their environmental applications and implications. Nanomaterials, 6(11), 209.

[63] Ebrahiminezhad, A., Zare-Hoseinabadi, A., Sarmah, A. K., Taghizadeh, S., Ghasemi, Y., & Berenjian, A. (2018). Plant-mediated synthesis and applications of iron nanoparticles. Molecular Biotechnology, 60(2), 154–168.

[64] Galdames et al., 2020 Zero-Valent Iron Nanoparticles for Environmental Applications.

[65] Natarajan, S., Harini, K., Gajula, G. P., Sarmento, B., Neves-Petersen, M. T., & Thiagarajan, V. (2019). Multifunctional magnetic iron oxide nanoparticles: Diverse synthetic approaches, surface modifications, cytotoxicity towards biomedical and industrial applications.

[66] Decaffmeyer, M., A. Thomas, and R. Brasseur, Les médicaments peptidiques: mythe ou réalité? BASE, 2008.

[67] Ung, D., Nanoparticules métalliques anisotropes synthétisées par voie chimique: fils, plaquettes et particules hybrides de cobalt-nickel, propriétés structurales et magnétiques; fils d'argent auto-organisés. 2005, Université Paris-Diderot-Paris VII.

[68] Balogoun, C.K., et al., Préparation des charbons actifs par voie chimique à l'acide phosphorique à base de coque de noix de coco. International Journal of Biological and Chemical Sciences, 2015. (1): p. 563-580.

[69] Arrisujaya, D., Yulizar, Y., & Saefumillah, A. (2025). Accelerated water purification with magnetite (Iron (II, III) Oxide) nanoparticles: Coagulation applications. J. Chem. Rev, 7(1), 25-62.

[70] Pasinszki, T., & Krebsz, M. (2020). Synthesis and application of zero-valent iron nanoparticles in water treatment, environmental remediation, catalysis, and their biological effects. Nanomaterials, 10(5), 917.

[71] Cao, J., Elliott, D., & Zhang, W. X. (2005). Perchlorate reduction by nanoscale iron particles. *Journal of Nanoparticle Research*, *7*(4), 499-506.

[72] Quinn, J., Geiger, C., Clausen, C., Brooks, K., Coon, C., O'Hara, S., ... & Holdsworth, T. (2005). Field demonstration of DNAPL dehalogenation using emulsified zero-valent iron. *Environmental science & technology*, *39*(5), 1309-1318.

[73] Suchak, N. M., Deshpande, M. P., Mistry, H. M., Bhatt, S. V., Pandya, S. J., Chaki, S. H., ... & Kunjadiya, A. P. (2025). Iron oxide nanoparticles embedded on activated carbon: a comprehensive investigation of photocatalytic, antibacterial, and anticancer properties. Physica Scripta, 100(7), 075969.

| Parameter Group | Parameter | Unit | Limit / Indicative Value |
|---|---|---|---|
| Chemical Parameters | Aluminium | mg/L | 0.2 |
| | Ammonium | mg/L | 0.5 |
| | Barium | mg/L | 0.7 |
| | Boron | mg/L | 1 (conventional water); 1.3 (desalinated/demineralized) |
| | Fluorides | mg/L | 1.5 |
| | Nitrates | mg/L | 50 |
| | Nitrites | mg/L | 0.2 |
| | Oxidability | mg/L $O_2$ | 5 |
| | Acrylamide | µg/L | 0.5 |
| | Antimony | µg/L | 20 |
| | Silver | µg/L | 100 |
| | Arsenic | µg/L | 10 |
| | Cadmium | µg/L | 3 |
| | Total Chromium | µg/L | 50 |
| | Copper | mg/L | 2 |
| | Cyanides | µg/L | 70 |
| | Mercury | µg/L | 6 |
| | Nickel | µg/L | 70 |
| | Lead | µg/L | 10 |
| | Selenium | µg/L | 10 |
| | Zinc | mg/L | 5 |
| | Total Polycyclic Aromatic Hydrocarbons (PAHs) | µg/L | 0.2 |
| | Benzo(a)pyrene | µg/L | 0.01 |

| | | | |
|---|---|---|---|
| | Benzene | µg/L | 10 |
| | Toluene | µg/L | 700 |
| | Ethylbenzene | µg/L | 300 |
| | Xylenes | µg/L | 500 |
| | Styrene | µg/L | 100 |
| | Methylene Blue Active Substances | mg/L | 0.2 |
| | Epichlorohydrin | µg/L | 0.4 |
| | Microcystin LR | µg/L | 1 |
| | Organochlorine Insecticides | µg/L | 0.1 |
| | Organophosphorus & Carbamate Insecticides | µg/L | 0.1 |
| | Herbicides | µg/L | 0.1 |
| | Fungicides | µg/L | 0.1 |
| | PCB | µg/L | 0.1 |
| | PCT | µg/L | 0.1 |
| | Aldrin | µg/L | 0.03 |
| | Dieldrin | µg/L | 0.03 |
| | Heptachlor | µg/L | 0.03 |
| | Heptachlor Epoxide | µg/L | 0.03 |
| | Total Pesticides | µg/L | 0.5 |
| | Bromates | µg/L | 10 |
| | Chlorite | µg/L | 0.07 |
| | Chloroform | µg/L | 200 |
| | Bromoform | µg/L | 100 |
| | Dibromochloromethane | µg/L | 100 |
| | Bromodichloromethane | µg/L | 60 |
| | Vinyl Chloride | µg/L | 0.3 |

| | | | |
|---|---|---|---|
| | 1,2-Dichloroethane | µg/L | 30 |
| | 1,2-Dichlorobenzene | µg/L | 1000 |
| | 1,4-Dichlorobenzene | µg/L | 300 |
| | Trichloroethylene | µg/L | 20 |
| | Tetrachloroethylene | µg/L | 40 |
| Radionuclides | Alpha Particles | pCi/L | 15 |
| | Beta Particles | mrem/year | 4 |
| | Tritium | Bq/L | 100 |
| | Uranium | µg/L | 30 |
| | Total Indicative Dose (TID) | mSv/year | 0.15 |
| Microbiological Parameters | Escherichia coli | n/100 mL | 0 |
| | Enterococci | n/100 mL | 0 |
| | Sulfite-reducing bacteria (including spores) | n/20 mL | 0 |
| Organoleptic Parameters | Colour | mg/L platinum | 15 |
| | Turbidity | NTU | 5 |
| | Odour at 25°C | Dilution ratio | 4 |
| | Taste at 25°C | Dilution ratio | 4 |
| | Alkalinity | mg/L $CaCO_3$ | 65 (minimum) |
| | Calcium | mg/L | 200 |

| | | | |
|---|---|---|---|
| Physico-chemical Parameters | Chloride | mg/L | 500 |
| | Hydrogen Ion Concentration (pH) | pH | 6.5–9 |
| | Conductivity at 20°C | µS/cm | 2800 |
| | Hardness (TH) | mg/L as $CaCO_3$ | 500 |
| | Total Iron | mg/L | 0.3 |
| | Manganese | µg/L | 50 |
| | Phosphorus | mg/L | 5 |
| | Potassium | mg/L | 12 |
| | Sodium | mg/L | 200 |
| | Sulfates | mg/L | 400 |
| | Temperature | °C | 25 |

**Maximum permissible limits for drinking water parameters**

| Parameter | Unit | Limit Value |
|---|---|---|
| Temperature | °C | 30 |
| pH | - | 6.5–8.5 |
| TSS | mg/L | 35 |
| Kjeldahl Nitrogen | mg/L | 30 |
| Total Phosphorus | mg/L | 10 |
| COD | mg/L | 120 |
| $BOD_5$ | mg/L | 35 |
| Aluminum | mg/L | 3 |
| ic Bioaccumulative Substances | mg/L | 0.005 |
| Cyanides | mg/L | 0.1 |
| Fluorides | mg/L | 15 |
| Phenol Index | mg/L | 0.3 |
| Total Hydrocarbons | mg/L | 10 |
| Oils and Greases | mg/L | 20 |
| Cadmium | mg/L | 0.2 |
| Total Copper | mg/L | 0.5 |
| Total Mercury | mg/L | 0.01 |
| Total Lead | mg/L | 0.5 |
| Total Chromium | mg/L | 0.5 |
| Tin | mg/L | 2 |
| Manganese | mg/L | 1 |
| Total Nickel | mg/L | 0.5 |
| Total Zinc | mg/L | 3 |
| Iron | mg/L | 3 |
| Total Organic Chlorides | mg/L | 5 |

**Algerian standards for liquid effluent discharge parameters (official journal of Algeria no.26,2006**

# Résumé

Ce travail vise à synthétiser des nanoparticules d'oxyde de fer ($Fe_3O_4$) par une approche verte basée sur des extraits végétaux, et à évaluer leur efficacité en tant que coagulant pour le traitement des eaux usées et des eaux de barrage. Dans un premier temps, les performances de ces nanoparticules ont été évaluées par des expériences de jar-test afin de déterminer la dose optimale de traitement. Par la suite, la meilleure condition obtenue a été sélectionnée, et un traitement complémentaire a été appliqué en combinant les nanoparticules résiduelles avec du charbon actif et un processus photocatalytique, dans le but de renforcer l'élimination des polluants. Les résultats ont démontré une amélioration significative de la qualité de l'eau traitée à différents niveaux, particulièrement dans la réduction de la charge organique et des nutriments, ainsi qu'une amélioration des paramètres microbiologiques. Cette étude confirme que les nanoparticules de ($Fe_3O_4$) synthétisées par voie verte représentent une approche efficace et prometteuse pour le traitement et l'amélioration de la qualité de l'eau dans une perspective de développement durable.

**Mots-clés :**

Nanoparticules de $Fe_3O_4$ ; Synthèse verte ; Extrait végétal ; Traitement des eaux ; Coagulation ; Charbon actif ; Photocatalyse ; Eaux usées ; Eau de barrage ; Élimination des polluants.

# ملخص

. تهدف هذه الدراسة إلى تخليق جسيمات أكسيد الحديد ($Fe_3O_4$)النانوية باستخدام طريقة خضراء تعتمد على المستخلصات النباتية، وتقييم كفاءتها كمخثر في معالجة مياه الصرف الصحي ومياه السدود. في البداية، تم تقييم أداء هذه الجسيمات النانوية من خلال تجارب اختبار الكأس (Jar-test) لتحديد الجرعة المثلى للمعالجة. بناءً على ذلك، تم اختيار الحالة الأفضل التي تم الحصول عليها، وتطبيق معالجة تكميلية باستخدام الجسيمات النانوية المتبقية مدمجة مع الكربون المنشط وعملية التحفيز الضوئي، بهدف تعزيز إزالة الملوثات. أظهرت النتائج تحسناً ملحوظاً في جودة المياه المعالجة على مستويات مختلفة، لا سيما في خفض الحمل العضوي والمغذيات، بالإضافة إلى تحسن في المؤشرات الميكروبية. تؤكد هذه الدراسة أن جسيمات ($Fe_3O_4$) النانوية المخلقة عبر مسار أخضر تمثل نهجاً فعالاً وواعداً لمعالجة المياه وتحسين جودتها ضمن منظور التنمية المستدامة

**الكلمات المفتاحية:**

جسيمات أكسيد الحديد النانوية($Fe_3O_4$) ؛ التخليق الأخضر؛ المستخلص النباتي؛ معالجة المياه؛ التخثير؛ الفحم النشط؛ التحفيز الضوئي؛ مياه الصرف الصحي؛ مياه السدود؛ إزالة الملوثات.

# Abstract

This work aims to synthesize iron oxide ($Fe_3O_4$) nanoparticles using a green approach based on plant extracts, and to evaluate their efficiency in the treatment of wastewater and dam water as a coagulant. First, the performance of these nanoparticles was assessed through jar-test experiments in order to determine the optimal treatment dose. Subsequently, the best obtained condition was selected, and a complementary treatment was applied using the residual nanoparticles combined with activated carbon and a photocatalytic process, with the aim of enhancing pollutant removal. The results demonstrated a significant improvement in treated water quality at different levels, particularly in the reduction of organic load and nutrients, as well as an improvement in microbiological parameters. This study confirms that $Fe_3O_4$ nanoparticles synthesized via a green route represent an effective and promising approach for water treatment and water quality improvement within a sustainable development perspective.

**Keywords:**

$Fe_3O_4$ nanoparticles; Green synthesis; Plant extract; Water treatment; Coagulation;

Activated carbon; Photocatalysis; Wastewater; Dam water; Pollutant removal.